LM - Laser Application

LM-0100 Michelson Interferometer

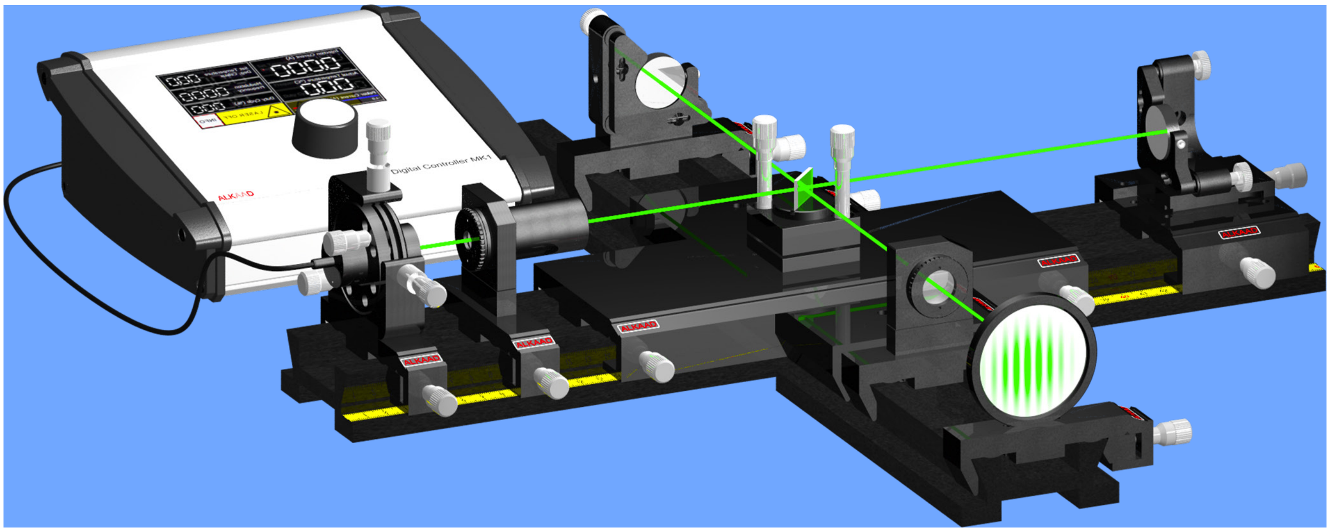

Keywords

DPSSL as coherent source
Fringe contrast
Spherical and plane waves
Properties of laser radiation
Coherence length
Two mode HeNe laser
Two beam interference
Fringe detection

Introduction

In 1881 A. A. Michelson constructed an interferometer, which later on also got his name, to counter prove successfully the theory of an universal ether assumed to be existing at that time. Later on he determined with this set-up the length of the basic meter in units of light wavelengths. Still, the promising use of interferometers in performing technical length measurements only reached significance after the discovery of the laser as a coherent light source. Today this contact less working high precision length measuring instruments have become an important tool for many areas of the machine building, industry like adjustment, final control, incremental displacement measurement for CNC machines, the control of machine tools and for calibration procedures. With the latest laser interferometers resolutions up to the nanometre range can be realised. The arrangement of the optical components has changed with regard to the original Michelson interferometer by the use of lasers as light sources. But with some exceptions, generally the two beam arrangements of Michelson is used. Within the frame of this experiment first the classical interferometer is setup and the interference pattern are observed on a screen. To understand the observed interference pattern the properties of Gaussian beams, wave fronts, radii of curvature and the superimposition of waves are discussed in the theoretical part of the manual. Starting with a simple model of monochromatic radiation, the spectral bandwidth of a light source will be considered and the influence on the contrast of the interferometer discussed. The coherence length is introduced, defined and measured.
The applied HeNe-Laser emits two orthogonally polarised modes with a coherence length of about 18 cm. In a second step the Michelson setup is upgraded to a technical interferometer.

How it works

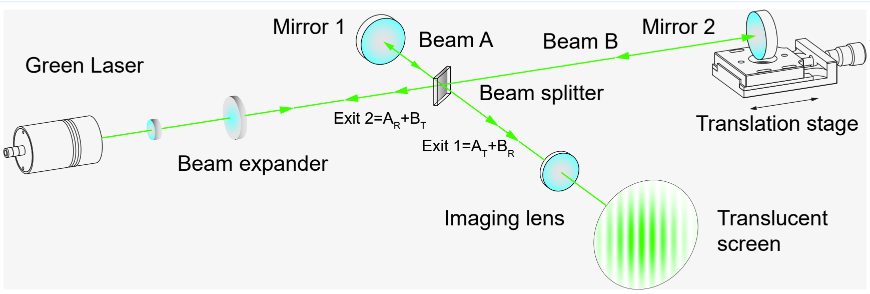

Fig. 2.1: The classical Michelson interferometer setup

The classical Michelson setup consists of the beam splitter, the mirror 1 and the mirror 2. The incident beam from a green laser is split into two beams at the beam splitter. The returning beams from mirror 1 and 2 are imaged by means of a diverging lens onto a translucent screen. Mirror 2 is mounted on a translation stage for precise change of the related optical path, particularly for white light interference. The beam expander provides an enlarged beam with plane wave fronts resulting in a fringe pattern with a parallel or circular pattern.

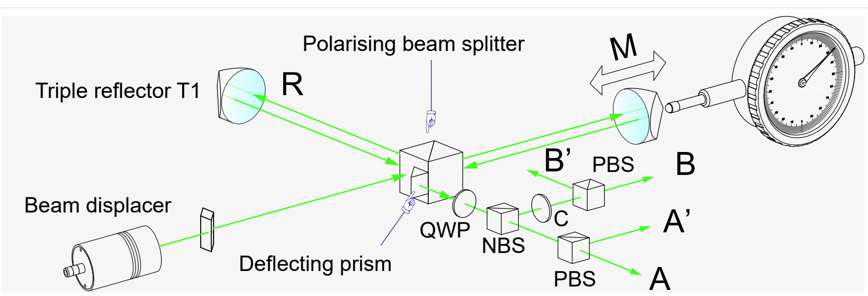

Fig. 2.2: The technical laser interferometer for length measurement

The technical interferometer is a refinement of the Michelson interferometer. To avoid any undesired back reflection into the laser source, triple reflectors are used instead of flat mirror. Furthermore the technical interferometer needs a mechanism for reliable counting of the fringes, even if the movement direction (M) is reversed. For this purpose optical quadrature signals are required. The superimposed waves of the reference arm (R) and (M) are leaving the interferometer at the deflecting prism. Both orthogonal linear polarised waves are converted into opposite circular polarisation by the quarter wave plate (QWP). In a next step the intensity is split into two equal parts, whereby one part travels to the channel (A) and the other to channel (B). In channel B a quartz polarizer turns the polarisation of channel B by 90° to channel A. In this way the required phase shift of 90° for the quadrature encoding is achieved. In addition, a polarizing beam splitter in each channel provides a 180° phase shift which is used to become independent of varying contrast of the moving interferometer.

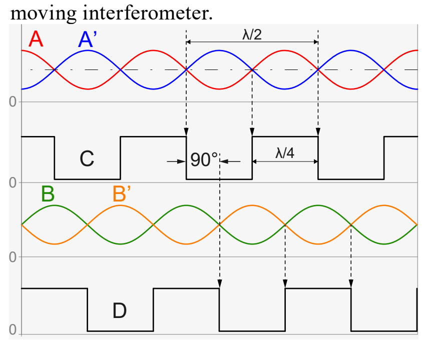

A comparator converts the A, A' and the B,B' into the quadrature signal C and D which are counted by a quadrature counter.

Description of the components

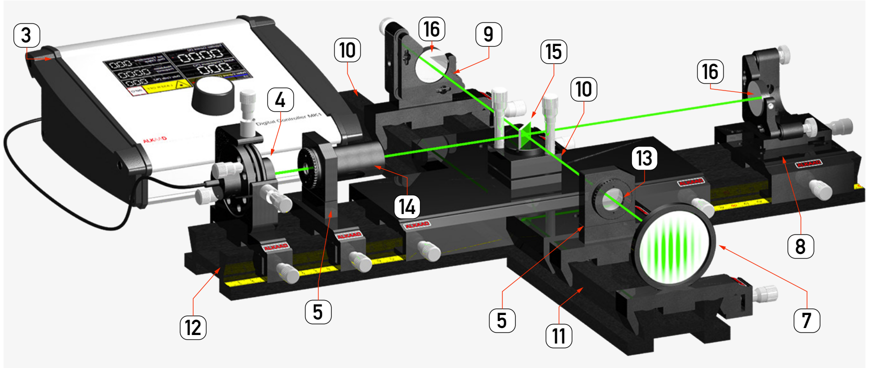

The Michelson interferometer is formed by the two mirrors (16) which are mounted into adjustable mounts (9). One mirror is mounted to a translation stage (8) attached to a carrier. The adjustable (10) beam splitter (15) divides and combines the beam of the green laser source (4) into two equal parts. The superimposed beams pass through the expansion lens (13) and are imaged onto the translucent screen (7) from which the pattern can be photographed by a simple digital camera. The light source is connected to the digital controller to provide the necessary current and temperature control. With the beam expander (14) the radius of curvature of the wave fronts can be changed from plane to spherical to create either stripes or circular interference pattern. From this interference pattern a photo can be taken by ordinary digital cameras of a smart phone and inserted into the student's report.
When moving the translation stage (8) the interference pattern changes accordingly. Real measurements can be carried out in combination with the technical extension (40). For the measurement of the index of a gas like air we recommend the "PE-0600 Optical Interferometer" on 75.

LM-0100 Michelson Laser Interferometer consisting of:

Item	*Code*	*Qty.*	*Description*	*Details page*
1	CA-0080	1	Optics cleaning set	128 (12)
2	CA-0450	1	BNC connection cable 1 m	130 (28)
3	DC-0040	1	Diode laser controller MK1	121 (4)
4	LQ-0040	1	Green (532 nm) stabilized Laser, 40 mW	119 (3)
5	MM-0020	2	Mounting plate C25 on carrier MG20	93 (1)
6	MM-0100	1	Target Cross in C25 Mount	94 (9)
7	MM-0110	1	Translucent screen on carrier MG20	94 (10)
8	MM-0444	1	Kinematic mount 1", translation stage on MG65	96 (28)
9	MM-0440	1	Kinematic mount C30 on MG20	96 (26)
10	MP-0050	1	Cross-piece MG-65 with kinematic mount ø 25mm	92 (1)
11	MP-0130	2	Optical Bench MG-65, 300 mm	93 (7)
12	MP-0150	1	Optical Bench MG-65, 500 mm	93 (8)
13	OC-0010	1	Biconcave lens f=-10 mm, C25 mount	98 (2)
14	OC-0380	1	Beam expander x8 in ø 25 mm housing	100 (18)
15	OC-0500	1	Beam splitter plate ø 25 mount	101 (29)
16	OC-1200	2	Laser mirror C30, ROC flat, HR @ 632 nm	107 (83)
17	UM-LM01	1	Manual Michelson Interferometer	
	Option (order separately)			
18	CA-0200	1	Oscilloscope 100 MHz digital, two channel	129 (19)
19	LM-0110	1	Two mode HeNe laser extension	see below

Two mode HeNe laser extension

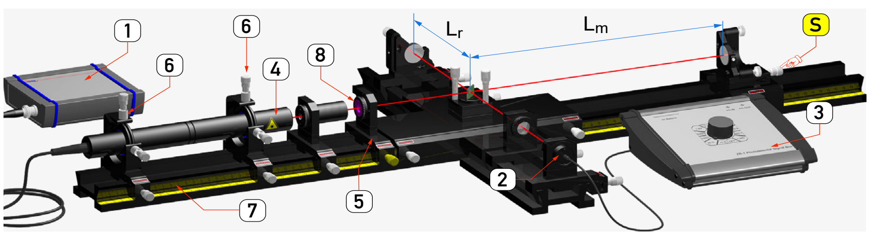

Based on the mode spacing of the two mode HeNe laser (4) the coherence length is 20 cm and can be determined by measuring the contrast as function of the path difference of the reference arm L_r and measuring arm L_m. By using a polarisation filter (8), one mode can be suppressed resulting in a single mode laser with much longer coherence length. The measurement starts with equal length of L_r and L_m .The path difference is increased in 1 cm steps and at each position the adjustment screw (S) is slightly turned back and forth while observing the oscilloscope which shows the signal of the photodetector (2). A more or less pure sine curve with varying amplitude and offset is observed (Fig. 2.3 and Fig. 2.4). The coherence length is reached at the position where the contrast reaches its minimum.

Measuring the contrast function and coherence length

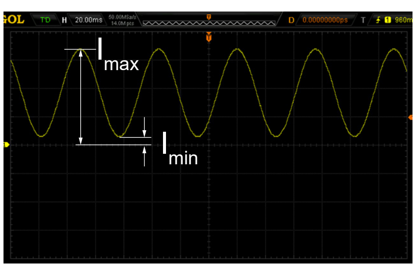

Fig. 2.3: Good contrast

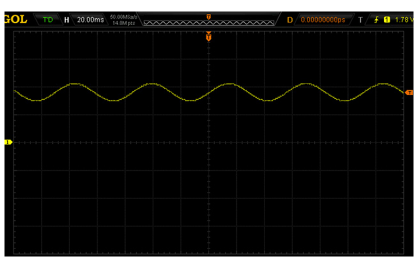

Fig. 2.4: Low contrast

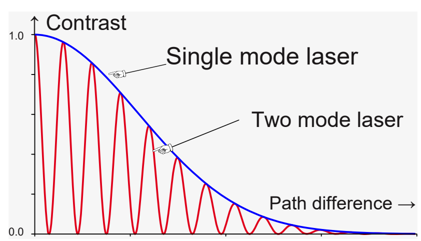

Contrast function

LM-0110 Two mode HeNe laser extension consisting of:

Item	*Code*	*Qty.*	*Description*	*Details page*
1	DC-0062	1	High voltage supply 5 mA	122 (8)
2	DC-0120	1	Si-PIN Photodetector, BPX61 with connection leads	123 (15)
3	DC-0380	1	Photodetector Junction Box ZB1	125 (31)
4	LQ-0300	1	Two mode HeNe laser Ø30 housing, 632 nm	120 (14)
5	MM-0024	1	Rotary mount on carrier MG20	93 (2)
6	MM-0470	2	XY mount, soft ring 30 mm, on MG20	97 (32)
7	MP-0150	1	Optical Bench MG-65, 500 mm	93 (8)
8	OC-0710	1	Polarizer in C25 mount	102 (34)

LM-0120 Technical Interferometer Add-on

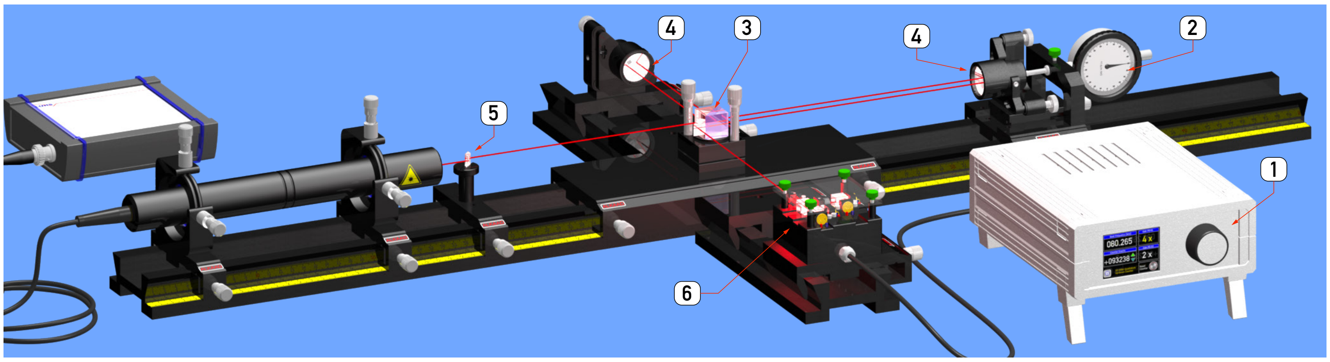

Laser Application

Keywords

Definition of Length | **HeNe-Laser** | **Two Beam Interference**

Homodyne Interferometer | **Fringe Detection and Counting** | **Interpolation of Interference Fringes**

Calibration of Micrometer Gauge

Introduction

One essential element of a technical laser interferometer is the secure detection of the bright to dark transitions (fringes) even for variable contrast conditions which may occur due to modifications of the initial adjustment during the displacement of the measuring reflector. To compensate for these influences a fringe signal A' with a phase shift of 180° with respect to fringe signal A is optically generated. By means of an subsequent electronic comparator, disturbing DC - offset parts are eliminated from the resulting signal. To detect the direction of the displacement of the measuring reflector a signal B, phase shifted by 90° with respect to signal A, is created optically. Furthermore such a 90° phase shifted signal D with respect to signal C is created. Also signal B and D are treated with a comparator to remove any offset. As a result two offset free fringe signals are created having a phase shift of 90° to each other allowing the directional discrimination by applying the quadrature encoder principle.
Another important difference against the classical Michelson interferometer lies in the fact that instead of mirrors, triple reflectors are used in such a way that no beam travels back into the laser source. Such back reflections lead to frequency and thus intensity fluctuation of the laser source falsifying the counted number of fringes.
This extension provides all necessary optical components to turn the existing Michelson interferometer to a technical one. One triple reflector is mounted onto a translation stage. The piston pin of the provided micrometer gauge firmly touches the back of the moveable triple reflector. The idea of the measurement is to calibrate the display of the gauge against the wavelength of the laser source which forms the secondary standard of a metre. The fringes generated by the movement are counted by the provided forward/backward counter in fractions of the wavelength λ like λ/4, λ/8 or even λ/16.

How it works

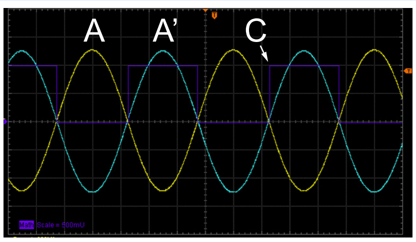

Fig. 2.5: Signals of channel A

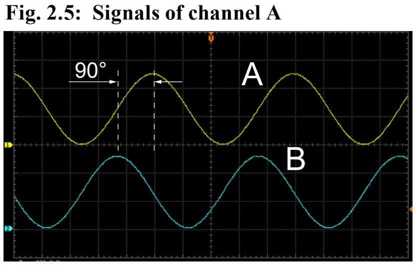

Fig. 2.6: Signals of channel A and B

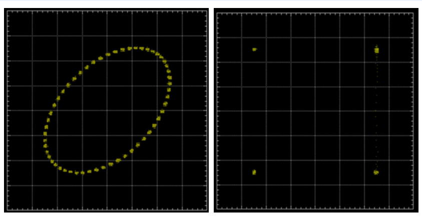

Fig. 2.7: Analogue and TTL A and B signals in XY representation

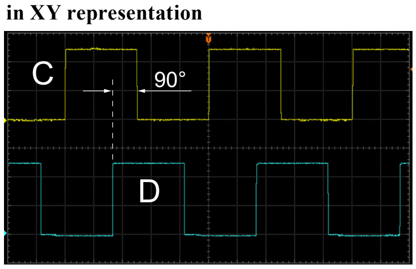

Fig. 2.8: Track of C and D TTL signals

The special feature of technical interferometer are the automated detection and counting of the fringes cause by a movement. In the Fig. 2.5 the signals A and A' (please refer to Fig. 2.2) are shown. From both signals the TTL signal C is generated. The Fig. 2.6 shows the phase shift of 90 degrees between the A and B signals (of course this shift exists also between the A' and B' signals). The XY oscilloscope representation of A and B is shown in the Fig. 2.7. The left figure shows the analogue superposition. If the system is in rest, only a dot on the circumference of the ellipse (ideally a circle) shows the position. A full turn is related to a travelled distance of λ/4 or 0.158 micrometer when λ is 635 nm and the rotation direction depends on the direction of movement. The right figure of Fig. 2.7 shows the XY representation of the TTL signals of C and D. Here, the dot jumps clockwise or counterclockwise from one corner to the other whereby one jump corresponds to a movement of λ/16. The task of the electronics is to count how many jumps occur in clockwise and in counterclockwise direction. This is achieved by using an up and down counter whereby the directional signal is gained from the 90° phase shift between both signals. If C leads D then the directional signal for the counter will be high (up) or low when D leads C.

LM-0120 Laser interferometer technical extension consisting of:

Item	*Code*	*Qty.*	*Description*	*Details page*
1	DC-0080	1	Quad counter & 2 channel photodiode amplifier	123 (11)
2	MM-0120	1	Dial gauge travel 5 mm resolution 1 µm on MG65	94 (12)
3	OC-0510	1	Polarising beam splitter cube on 25 mm stage	101 (30)
4	OC-0520	2	Triple reflector in extended 1" mount	101 (31)
5	OM-0040	1	Beam displacer 5 mm on MG20	111 (5)
6	OM-0840	1	Fringe detection unit on MG100	117 (43)
	Option (order separately)			
7	MM-0140	1	Triple reflector on motorised translation stage, travel 50 mm	94 (13)
	Required Option (order separately)			
8	CA-0200	1	Oscilloscope 100 MHz digital, two channel	129 (19)

LM-0140 CNC Calibration Extension

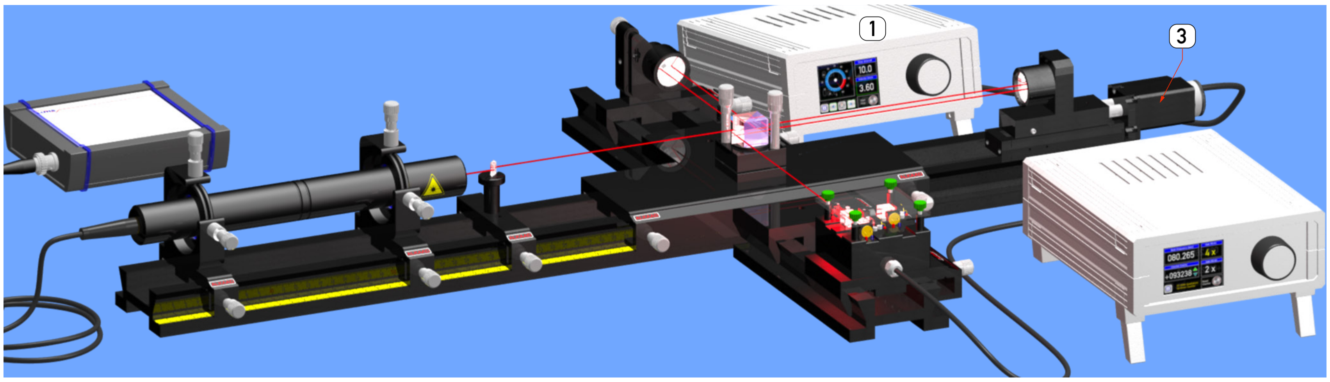

Definition of Length | **HeNe-Laser** | **Two Beam Interference**
Homodyne Interferometer | **Fringe Detection and Counting** | **Interpolation of Interference Fringes**
Computer controlled stepper motor | **Calibration of Translation Stage**

Measuring a length is the comparison of an unknown length with a known one. Since 1983 the standard of one meter is defined as the length of the path travelled by light in vacuum during a time interval of 1/299792458 of a second. The effect of this definition is to fix the speed of light (c) in vacuum at exactly 299 792 458 m/s. If we consider the relation $\nu=c/\lambda$ where ν denotes the frequency and λ the wavelength of the light radiation, it becomes clear that in case the frequency of the radiation is known, the wavelength λ is known as well. If the used light source has a known and constant frequency it represents a secondary standard of the meter. Preferentially a laser can fulfil the demand of a defined and stable frequency. In practise HeNe-Laser systems are used whose frequency is stabilised using optical transitions of the Iodine 127 isotope. The uncertainty of the frequency stabilisation by using this method is better than $1x10^{-12}$. For technical applications like calibrating CNC machines an uncertainty of $1x10^{-7}$ is sufficient. This value corresponds to an accuracy of 0.1 µm per one meter. A HeNe-Laser without any means of frequency stabilisation has a fairly good uncertainty of $1x10^{-6}$ and will be used in this experiment. By using the Michelson interferometer we count how many $\lambda/2$ bright/dark transitions (fringe) occur along the distance to be measured. The movement will be done by using a microprocessor controlled motorised translation stage. The travelled distance is compared with the result of the Michelson interferometer which represents the secondary standard of the meter.

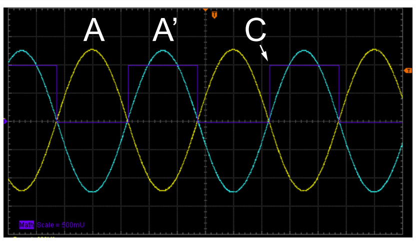

Fig. 2.9: Signals of channel A

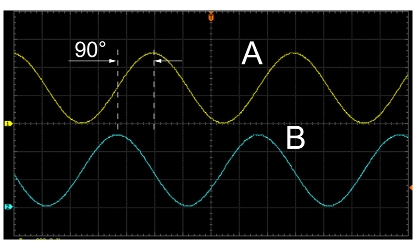

Fig. 2.10: Signals of channel A and B

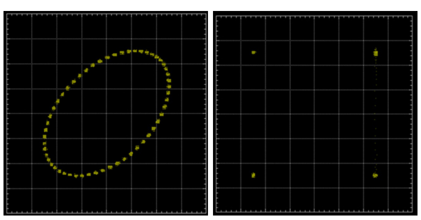

Fig. 2.11: Analogue and TTL A and B signals in XY representation

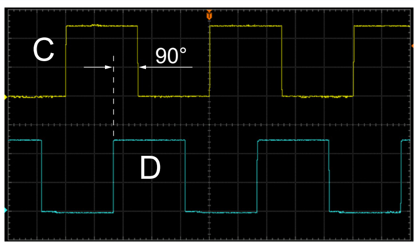

Fig. 2.12: Track of C and D TTL signals

The special feature of technical interferometer is the automated detection and counting of the fringes caused by a movement. In the Fig. 2.9 the signals A and A' (please refer to Fig. 2.2) are shown. From both signals the TTL signal C is generated. The Fig. 2.10 shows the phase shift of 90 degrees between the A and B signals (of course this shift exists also between the A' and B' signals). The XY oscilloscope representation of A and B is shown in the Fig. 2.11. The left figure shows the analogue superposition. If the system is in rest, only a dot on the circumference of the ellipse (ideally a circle) indicates the position. A full turn is related to a travelled distance of $\lambda/4$ or 0.158 micrometer when λ is 635 nm and the rotation direction depends on the direction of movement. The right figure of Fig. 2.11 shows the XY representation of the TTL signals of C and D. Here, the dot jumps clockwise or counterclockwise from one corner to the other whereby on jump corresponds to a movement of $\lambda/16$. The task of the electronics is to count how many jumps occur in clockwise and in counterclockwise direction. This is achieved by using an up and down counter whereby the directional signal is gained from the 90° phase shift between both signals. If C leads D then the directional signal for the counter will be high (up) or low when D leads C.

The movement of the translation stage (3) is controlled by the stepper motor controller (1). The increment as well as the speed is set to suitable values. After each increment the controller stops the movement for a while and the counted fringes are read from the counter display. Either the microprocessor or the student calculates the travelled distance from the counted fringes and creates a graph as shown in Fig. 2.13.

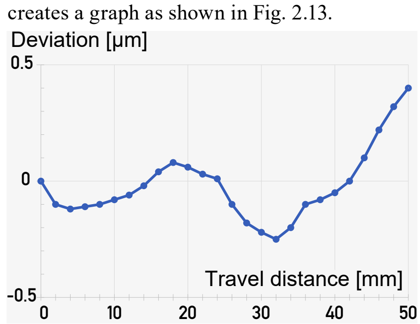

Fig. 2.13: Calibration curve

When using an extra computer the Fig. 2.13 can be automatically recorded by using the control and logger software (2). In this case the counter as well as the stepper motor controller are connected via the USB bus to the computer.

LM-0140 CNC Calibration Extension consisting of:

Item	*Code*	*Qty.*	*Description*	*Details page*
1	DC-0100	1	Stepper motor controller	123 (13)
2	ES-0200	1	Interferometer control and logger software	
3	MM-0140	1	Triple reflector on motorised translation stage, travel 50 mm	94 (13)

LM-0200 Zeeman Laser Frequency Stabilisation

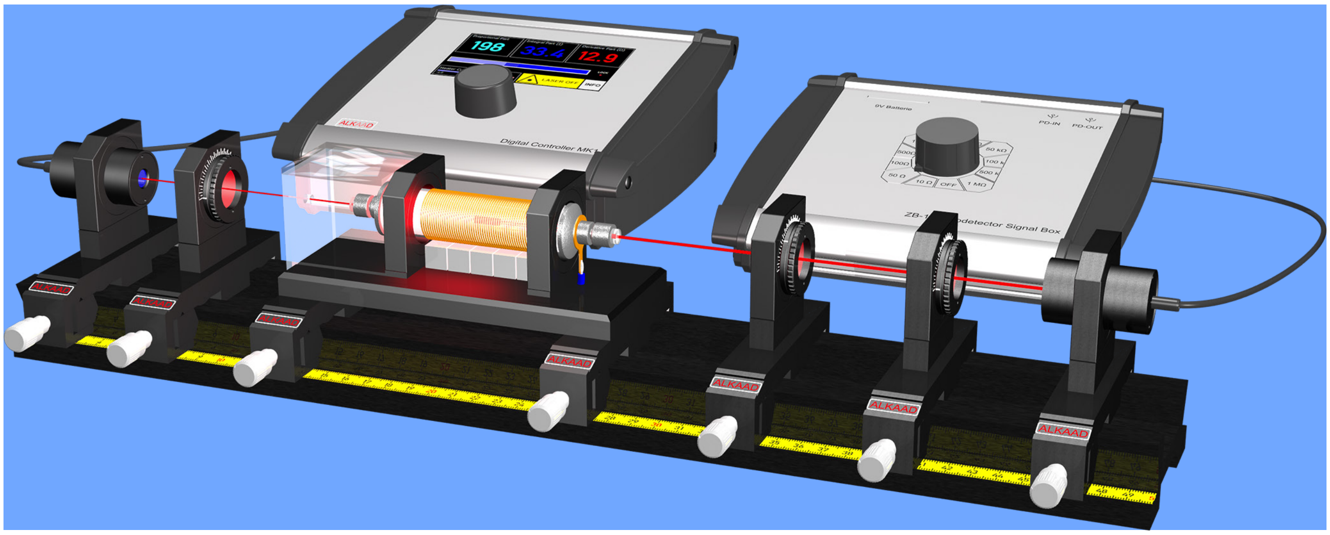

Keywords

Single Mode HeNe-Laser
Beat Frequency
Circular Laser Polarisation
Doppler Gain Profile
PID - Controller
Frequency Pulling
Longitudinal Zeeman Effect

Introduction

In principle the frequency of a laser is defined by its own intrinsic parameters. However in reality the emission frequency f is not stable within a couple of hours. For high precision interferometric length measurements at least a long term stability of $df/f \leq 10^{-8}$ must be provided within 8 hours. To obtain such a performance a stabilisation loop must be added to the Laser. Within this setup the Zeeman stabilisation - the most commonly used technique - of a HeNe-Laser is applied and demonstrated. The length of the HeNe laser tube is chosen in such a way that only a single mode can oscillate. A longitudinal magnetic field is applied to the HeNe tube and the normal linearly polarised splits into two oppositely circular polarised modes due to the Zeeman effect. One can observe the difference or beat frequency with a photodetector behind a polarizer. The beat frequency becomes minimum, when the HeNe laser tube (cavity) is aligned to the centre of the gain profile. The control loop consists of the beat frequency detection and an embedded micro processor based PID - controller. The active actuator is formed by a bifilar heater coil surrounding the laser tube. The task of the students is to understand the stabilisation concept and the underlying control technique of a PID controller. The PID parameter can be set independently from each other and the student will recognize the influence of this parameter on the control loop. The provided software records and displays the controller as well as laser response allowing to record a Bode diagram or the beat frequency drift of the free running laser.

How it works

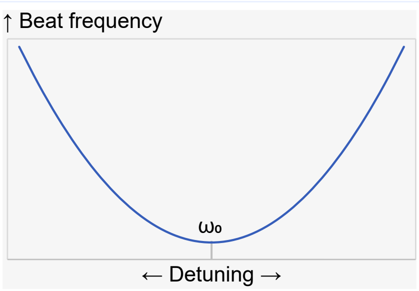

Fig. 2.14: Beat frequency of the Zeeman split laser modes versus the cavity detuning

In 1964 Culshaw and Kannelaudl investigated the effects of a longitudinal magnetic field on a He-Ne laser. Later in 1980 T. Baer et. al. published in his paper “Frequency stabilization of a 0.633 µm He-Ne longitudinal Zeeman laser“ the idea of a stabilization technique which provided a high frequency stability of $<10^{-9}$ independent on the aging effects of a HeNe laser tube. The name of the paper already suggests the use of the Zeeman effect in a laser. Within the experiment we will also focus on the Zeeman effect which normally requires in the classical experiments comparatively strong magnetic fields (500 mT) to obtain an observable effect. In the case of the HeNe laser already quite moderate magnetic field of 5 mT yields a beat frequency of around 300 kHz, thus the observation of the Zeeman effect is quite simple. However, the explanation is quite complex due to the manifold of involved laser effects. Due to the longitudinal nature of the Zeeman effect one would expect that the laser will now oscillate on two circular polarised modes with a frequency difference which is determined by the magnetic field. As the experimental results will tell us, it is a bit more complicated.

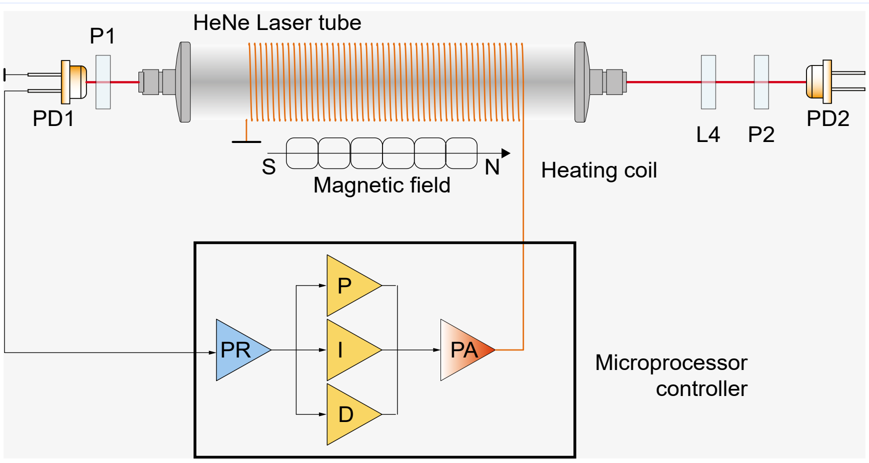

Fig. 2.15: Principle of the Zeeman frequency stabilised laser

The length of the laser tube is designed in such a way, that only one longitudinal mode oscillates. Applying a longitudinal magnetic filed causes at first the splitting of all the atomic energy level, in particular also the level of the Ne - laser transition. This causes the emission of two orthogonally circular polarized modes with a certain beat frequency. By means of the photodetector (PD1) behind the under 45° oriented polarizer (P1) this beat frequency is detected and displayed on an oscilloscope for instance. The microprocessor records the drift of the beat frequency and determines the minimum value which is related to the target of the control circuit. In some further steps the microprocessor learns if it needs to heat or cool to achieve the right control direction. Once these parameters are settled and the initial thermal drift of the tube slowed down, the controller starts the active control.

Description of the components

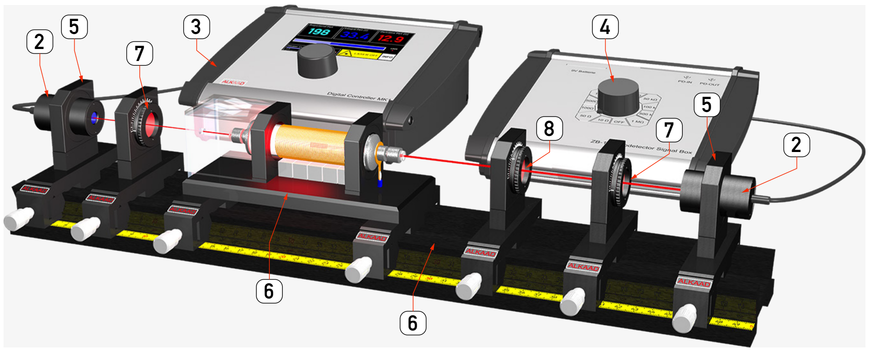

The Helium Neon Laser tube is operated by a compact high voltage supply (1). The anode is covered by a Perspex cover to avoid electrocution under all circumstances. The main laser beam with a maximum power of 1 mW leaves the tube at the opposite side, whereas through a small hole at the anode side a weak laser beam is used for the detection of the beat frequency.

The polarizer (7) on the left side is set under an angle of 45° to convert the opposite circular polarised laser beam into linear polarized light which is detected by the photodetector (2). A longitudinal arranged magnet array causes the Zeeman splitting and the bifilar heating coil is used to control the length of the HeNe laser tube. The stabilizer controller amplifies the beat frequency signal coming from the attached photodetector. The control strategy is based on sampling the beat frequency during the heat up. Hereby the laser drifts over a manifold of orders providing solid information about the minimum of the beat frequency which in fact is the control target. To achieve the best controller performance, the PID parameter needs to be determined and applied.

Once these tasks are accomplished, the main laser output is analysed. As already mentioned it consists out of two opposite circular polarised modes. To prove this, a rotatable quarter wave plate (8) converts the circular polarised modes into linear ones. With the polarizer (7) behind the quarter wave plate these two orthogonal modes are verified. The junction box (4) converts the photocurrent of the photodetector into a voltage which can be measured by a simple digital voltmeter or displayed on the oscilloscope to show the beat frequency of the modes. .

Measurements

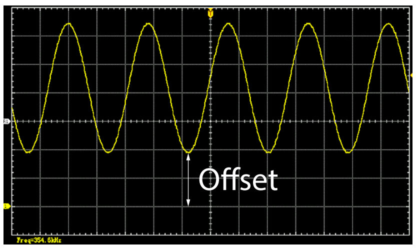

Fig. 2.16: Beat frequency measurement

The beat frequency signal can either be taken from the stabilisation controller (3) or the junction box (4). The Fig. 2.16 shows an oscilloscope screen dump. The signal shows an offset which is caused by non perfect polarizer as well as caused by the laser. However, using a pure AC amplifier removes the offset completely. A clear picture can be taken only once the thermal drift slows down or even better when the controller has been locked to the stabilisation point.

Control Software

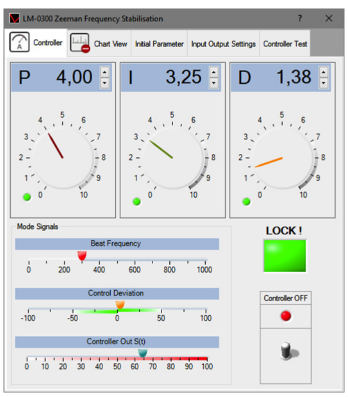

Fig. 2.17: Controller settings

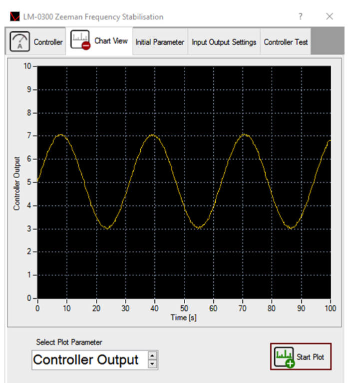

Fig. 2.18: Y-t plot and chart area

The controller (3) has a USB interface to communicate with a Windows based computer. The provided software (13) allows the set of the PID controller parameters to optimise the control accuracy. The Fig. 2.17 shows the screen where the individual control parameter are set. Three gauges give dynamic information about the beat frequency, the control deviation and the controller output which controls the heating coil current. In case the deviation tends to zero the “LOCK” has been reached. The Fig. 2.18 shows another page of the software, the chart recorder which is used for recording the controller output or the beat frequency as function of the time. The curve shown in Fig. 2.18 shows the controller output as function of the time. The parameters have been set to allow the controller to oscillate. From the period of the signal we get information about the control loop’s dead time and can predict control parameter (PID) for the optimum control accuracy. This method based on the Bode’s plot provides already good values, however, the parameter need further refinement while observing the controller.

LM-0200 Zeeman Laser Frequency Stabilisation consisting of:

Item	*Code*	*Qty.*	*Description*	*Details page*
1	DC-0064	1	High voltage supply 6.5 mA	122 (9)
2	DC-0120	2	Si-PIN Photodetector, BPX61 with connection leads	123 (15)
3	DC-0310	1	Laser frequency stabilizer	125 (27)
4	DC-0380	1	Photodetector Junction Box ZB1	125 (31)
5	MM-0020	2	Mounting plate C25 on carrier MG20	93 (1)
6	MP-0150	1	Optical Bench MG-65, 500 mm	93 (8)
7	OM-0400	2	Rotary Polariser / Analyser 360° on Carrier 20 mm	112 (15)
8	OM-0410	1	Rotary quarter wave plate on carrier	112 (16)
9	OM-0910	1	Single Mode HeNe laser with Zeeman magnet	117 (44)
10	UM-LM02	1	Manual Laser frequency stabilisation	
	Option (order separately)			
11	CA-0120	1	Tablet PC Windows	128 (15)
12	CA-0200	1	Oscilloscope 100 MHz digital, two channel	129 (19)
13	ES-0300	1	PID Controller Software	

Highlights

Basic and advanced level ★★★★ experiments

Outstanding features:

- ★★★ Zeeman effect
- ★★ Ultra stable laser frequency
- ★★ Controller PID trimming

Intended institutions and users:

- Physics Laboratory
- Engineering department
- Electronic department
- Biophotonics department
- Physics education in Medicine

LM-0300 Fabry Perot Spectral Analyser

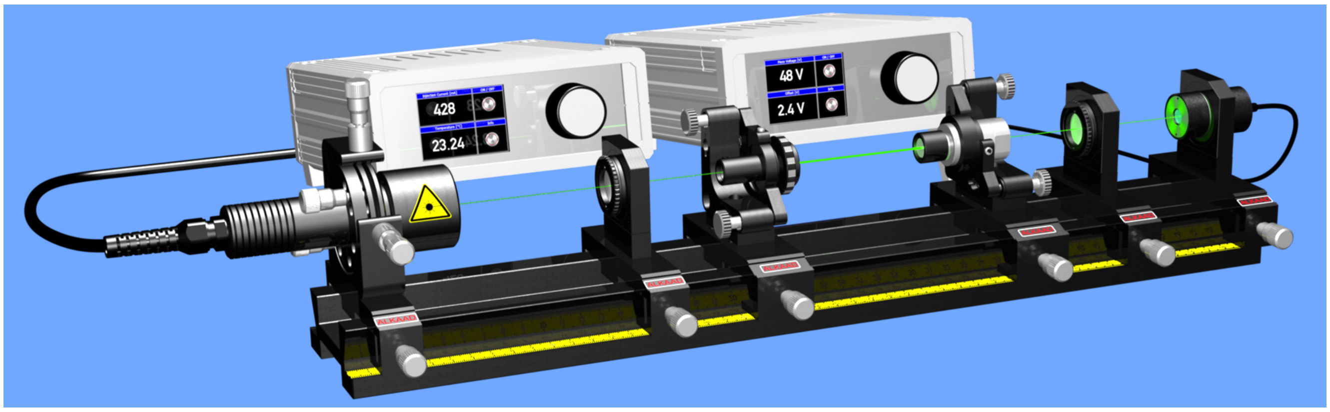

Keywords

Multiple Beam Interference
Visibility
Stability Criterion
Confocal Cavity
HeNe two mode probe laser
Finesse
Coherence length
Spectral Analysis
Hemispherical cavity
Free Spectral Range
Ideal & Real Fabry Perot
Flat mirror
DPSS single mode probe laser

Introduction

This experiment shows the properties of optical resonators especially the „Fabry Perot" (FP) resonator which is the most important of all stable laser resonators. The properties and behaviour of such a resonator will be discussed and measured as well as the resonance condition, the free spectral range and finesse. The stability criteria of confocal, hemispherical and plane parallel resonator types are calculated and measured. Finally, the resonator will be used as a spectrum analyser, a so called scanning Fabry Perot. The mode spectra of the provided green single mode diode pumped solid state laser (DPSSL) and optional two mode HeNe-laser is measured. The resonator mirrors are mounted in precision adjustment holders. One mirror is mounted on a low voltage piezo-electric transducer (PZT) which is controlled in amplitude and frequency by means of a voltage (0-150 V) controller. The other one is mounted into a precise translation element to achieve the perfect confocal match for curved mirror. The PZT periodically changes the length (0 to 10 µm) of the cavity sweeping over some resonances. The signal of the photodiode and the triangular PZT scanning amplitude are displayed on an oscilloscope showing the Airy function for some resonances. By using the known distance of the FP mirror, the free spectral range is determined and is used to calibrate the horizontal axis of the oscilloscope as the distance of two recurring peaks (Fig. 2.20). The mode spectra of the DPSSL - Laser is measured and interpreted by this method. Surprisingly, the green emitting DPSSL emits a very pure single mode if the temperature and injection current are properly controlled. In addition, an optional two mode HeNe probe laser can be used to measure the mode spacing with the SFP. Some parts of this experiment can also be used in connection with the experimental HeNe-Laser, to demonstrate the single mode operation, when an etalon is used inside of its cavity. By tuning it, even the gain profile of the HeNe-laser can be measured.

How it works

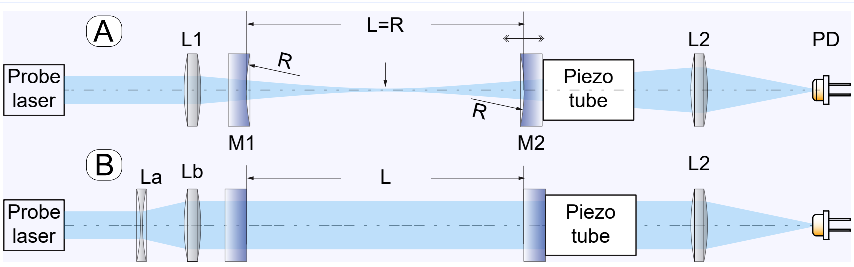

Fig. 2.19: Principle of a scanning Fabry Perot (A) spherical (B) plane mirror

The classical Fabry Perot (FP) uses two flat mirrors having a fixed distance L to each other. If the mirrors are coated to the surfaces of a highly precise parallel ground and polished glass cylinder such a device is termed as Fabry Perot Etalon. Such a static FP creates a circular interference pattern and its ring structure of it carries the spectral information of the incident light. Another class of a Fabry Perot is the scanning Fabry Perot (SFP). In this case the mirrors are separated, whereby one mirror is mounted to an element which periodically moves the mirror back and forth. The static Airy function which describe the transmittance of a FP becomes now also a function of time t.

$$T = \frac{1}{1+F\cdot\sin^2\left(\frac{\pi}{\lambda}\cdot n\cdot L\right)} \rightarrow T(t) = \frac{1}{1+F\cdot\sin^2\left(\frac{\pi}{\lambda}\cdot n\cdot L(t)\right)}$$

F stands for the finesse, λ for the wavelength, n for the index of refraction of the media between the mirror and L as distance of the two mirrors. The modulation of the length $L(t)$ is usually done with a PZT the length of which changes depending on the applied voltage. The transmission becomes maximum if the sin^2 term in the Airy function is zero. This is the case for $L(t)=N\cdot\lambda/2$, whereby N is an integer number. The range for N → N+1 is the range between two consecutive transmission peaks and is called free spectral range (FSR).

$$FSR \rightarrow \delta v = \frac{c}{2\cdot L}$$

We are using δv as frequency rather than $\delta\lambda$ because it is more convenient. The FSR is a very important value as it allows the calibration of the time axis of the graph of Fig. 2.20. The finesse F is determined as FSR/FWHM and its value is a parameter for the resolution of the FP. The finesse of a FP depends on the reflectivity of the mirror. However the flatness of the mirrors are even more important. In practice it turns out that the use of flat mirrors creates some disadvantages.

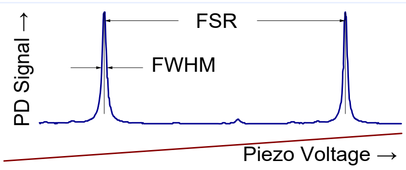

Fig. 2.20: Typical SFP measurement

Firstly, the alignment of absolute parallelism of both mirrors is hard to achieve and secondly the flatness of the mirror must be very accurate (better than λ/10). The case (B) of Fig. 2.19 shows the setup for such a plane mirror SFP. To reduce the limiting effect of the flatness imperfections, the beam of the probe laser is expanded (La and Lb). To dilute the high demand for precise alignment a SFP with spherical mirror is used. Due to the curved mirror the photons are redirected to stay inside the SFP. For a plane mirror already a small deviation of the parallel aligned mirrors lets the photons leave the cavity after a couple of round trips. In case (A) of Fig. 2.19 such a spherical SFP is shown. The best results are obtained if the mirror are positioned such that their distance $L=R$ *(confocal)*. Since mirror M1 acts as concave lense the mode matching lens (L1) compensates this effect. As for all spherical cavities higher transverse modes can occur, thereby falsifying the measurement. The transverse modes vanish if the distance L is exactly aligned to R. For this purpose M1 is mounted onto a precise translation element which can be varied by a few mm.

Static Fabry Perot

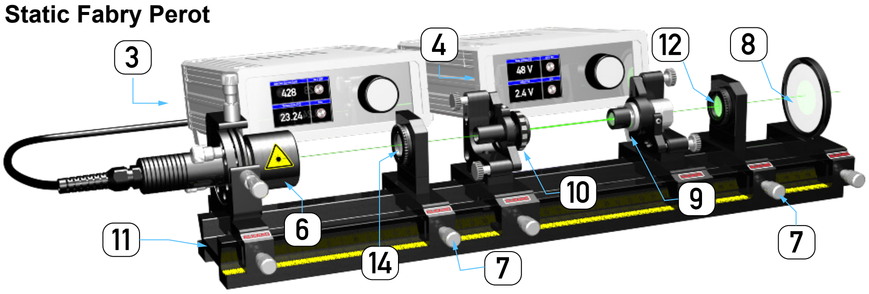

Fabry Perot with white screen to visualise static interference pattern

The experimental work may start with the static Fabry Perot: that means the PZT is not active. In a first alignment step, the beam of the probe laser is aligned collinear to the mechanical axis of the setup. As visual aid the biconcave lens (12) and the translucent screen (8) are used. The beam of the green probe laser (6) passes the mode matching lens (14) and enters the Fabry Perot consisting of (10) and (9). In (10) the mirror (16) is mounted and in the PZT of (9) the mirror (14) is mounted. The distance of the mirror should be exactly 75 mm which is the radius of curvature of the mirrors (15 and 16). A coarse alignment is done by using the ruler attached to the rail (11). While observing the occurring interference structure on the translucent screen (8) the adjustment of the Fabry Perot is improved. To align the distance of the mirror to reach the confocal case, the precision translation of (10) is used. By turning the knob the mirror is precisely moved back or forth. The confocal case is achieved when the interference pattern shows the highest contrast and clarity. Photographs of the pattern can be taken from the rear of the translucent screen. Static pattern tell a lot about the Fabry Perot as well as about the mirror quality. The figure below has been taken from the translucent screen. Some areas are showing a dark structure interrupting the regular circular image which is due to surface deviations of the spherical mirror from a perfect sphere. Due to the huge number of reflexions even very small deviations will create such visible contrast deformations.

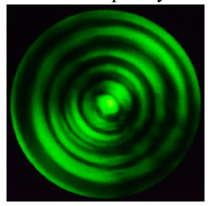

Dynamic Fabry Perot

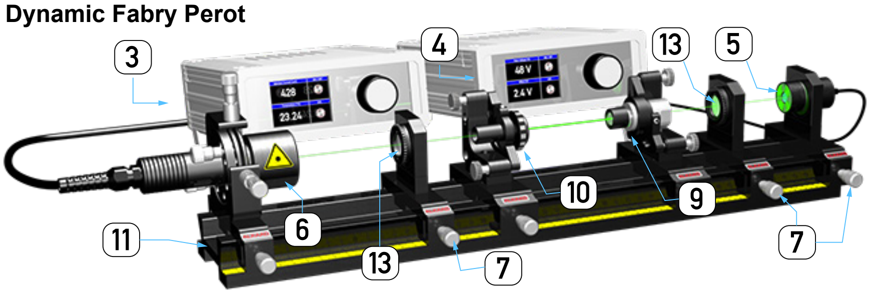

Fabry Perot with photodetector to take the dynamic interference pattern

By exchanging the expanding lens (12) with the focusing lens (13) with a focal length of 60 mm and replacing the translucent screen with the mounting plate (7) including the photodetector (5) the setup is ready for dynamic measurements. The photodetector is connected to the controller (4) which also contains the controller for the PZT. The amplified photodiode signal from the controller is connected via the provided BNC cable to an oscilloscope (22). In the same way the PZT voltage signal is connected to the second channel of the oscilloscope and serves also as trigger source. At the beginning a modes spectrum shown in Fig. 2.21 will be obtained. It shows a number of transverse extra peaks beside the main longitudinal mode. The transverse modes do not stem from the probe laser, they are eigenmodes of the Fabry Perot. These modes vanish once the confocal case is aligned and the cavity axis is collinear to the incident probe laser beam. The Fig. 2.22 shows the oscilloscope image of a well aligned confocal Fabry Perot. The FSR $\delta\nu$ for the confocal Fabry Perot is given by $\delta\nu=c/4R$ which yields for a radius of curvature R=100 mm of the mirror of a value 750 MHz. From Fig. 2.22 we further estimate the finesse of about 50 and a line width (FWHM) of 15 MHz. From this point we can conclude, that the line width of the probe laser is ≤ 15 MHz. The coherence length L_c of a laser source is related to $L_c=c/\Delta\nu$ with c as speed of light and $\Delta\nu$ the line width yields 20 metre, which is an astonishingly large value for a green laser pointer!

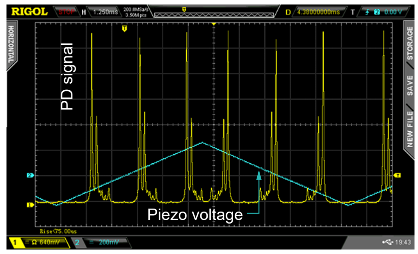

Fig. 2.21: Mode spectrum with transverse modes

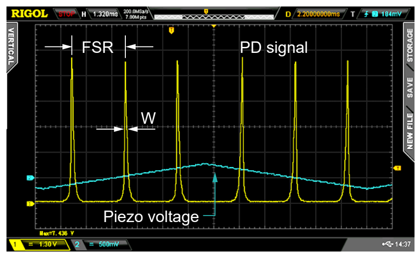

Fig. 2.22: Pure Single mode spectrum of the green probe laser

LM-0300 Fabry Perot Spectrum Analyser consisting of:

Item Code Qty. Description Details page

Item	*Code*	*Qty.*	*Description*	*Details page*
1	CA-0080	1	Optics cleaning set	128 (12)
2	CA-0450	3	BNC connection cable 1 m	130 (28)
3	DC-0010	1	Diode laser controller MK1-HP	121 (1)
4	DC-0070	1	Piezo controller 0-150V	122 (10)
5	DC-0120	1	Si-PIN Photodetector, BPX61 with connection leads	123 (15)
6	LQ-0040	1	Green (532 nm) stabilized Laser, 40 mW	119 (3)
7	MM-0020	3	Mounting plate C25 on carrier MG20	93 (1)
8	MM-0110	1	Translucent screen on carrier MG20	94 (10)
9	MM-0500	1	Piezo transducer 10µ/150V in kinematic mount	97 (36)
10	MM-0510	1	Kinematic mount with axial translation on MG30	98 (38)
11	MP-0100	1	Optical Bench MG-65, 1000 mm	92 (4)
12	OC-0005	1	Biconcave lens f=-5 mm, C25 mount	98 (1)
13	OC-0060	1	Biconvex lens f=60 mm in C25 mount	99 (5)
14	OC-0152	1	Biconvex lens f=150 mm in C25 mount	99 (11)
15	OC-1096	1	Laser mirror M12, ROC 75 mm, T 4% @ 532 and 632 nm	106 (70)
16	OC-1098	1	Laser mirror M22, ROC 75 mm, T 4% @ 532 and 632 nm	106 (71)
17	UM-LM03	1	Manual Fabry Perot Resonator	
	Option (order separately)			
18	LM-0310	1	Fabry Perot Advanced Accessories Upgrade Kit	46
19	LM-0330	1	Two Mode HeNe Laser Extension Kit	47
	Required Option (order separately)			
20	CA-0200	1	Oscilloscope 100 MHz digital, two channel	129 (19)

Highlights

Premium class experiment
Use of high precision DPSSL
Precise confocal adjustment
Low voltage prestressed PZT
Two wavelength 532 and 632 nm operation
Static transverse modes pattern

Intended institutions and users:
Advanced
Physics Laboratory
Engineering department
Electronic department

LM-0310 Fabry Perot Advanced Accessories Upgrade Kit

This upgrade kit adds an achromatic lens (1) which in combination with the "OC-0005 Biconcave lens f=-5 mm, C25 mount" and respective mounts becomes a 6 x beam expander. Such an expander is required when using the Fabry Perot with flat mirrors. Without such an expander sufficient finesse is not obtained.. For the experiments with flat mirrors the items (4) and (5) are needed. The mirrors (2, 3) have a radius of curvature of 100 mm resulting in a free spectral range of 750 MHz. It should be noted that the two modes of the HeNe-laser with its mode spacing of 730 MHz will not be resolved when operating the Fabry Perot with this mirror. The reason to use this mirrors is to challenge the students and give a more deeper understanding of a Fabry Perot.

LM-0310 Fabry Perot Upgrade Kit consisting of:

Item	*Code*	*Qty.*	*Description*	*Details page*
1	OC-0120	1	Achromat f=20 mm in C25 mount	99 (8)
2	OC-1010	1	Laser mirror M22, ROC 100 mm, T 4% @ 532 & 632 nm	106 (72)
3	OC-1012	1	Laser mirror M12, ROC 100 mm, T 4% @ 532 & 632 nm	104 (60)
4	OC-1090	1	Laser mirror M22, ROC flat, T 4% @ 532 and 632 nm	105 (68)
5	OC-1094	1	Laser mirror M12, ROC flat, T 4% @ 532 and 632 nm	106 (69)

LM-0330 Two Mode HeNe Laser Extension Kit

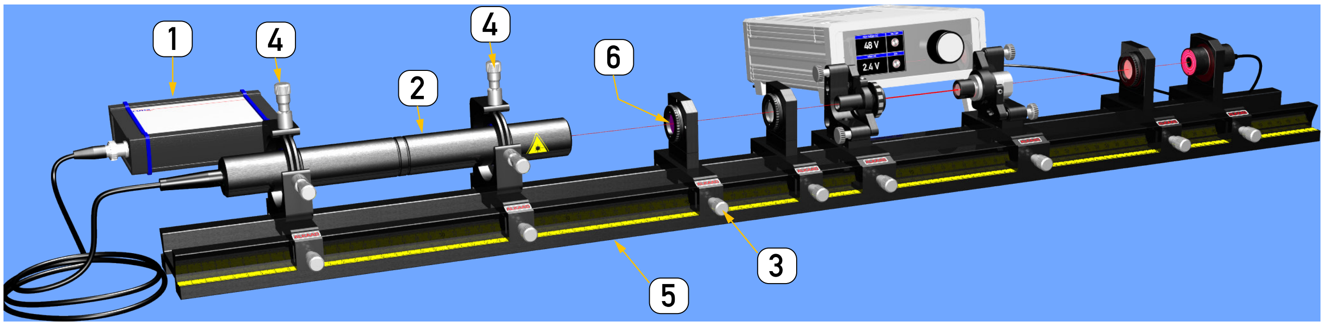

Two Mode HeNe - Laser
Orthogonal Modes

Mode Spacing 730 MHz
Mode Sweeping, Gain Profile

Linear Polarisation
Transverse Fabry Perot Modes

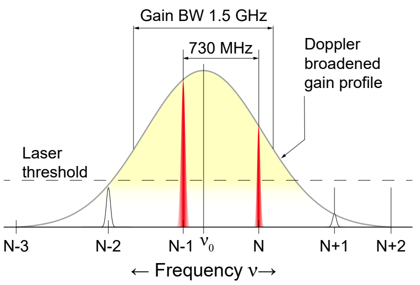

Fig. 2.23: HeNe-laser gain profile

The Helium Neon laser provides highly coherent and stable emission. This kit is intended as extension of the Fabry Perot LM-0300 which comes with a highly coherent DPSSL. The length of the HeNe-laser tube is designed in such a way that only two linearly polarised modes are emitted. The mode spacing is 730 MHz and the modes are orthogonally polarised to each other. By means of an external polarizer one of the modes can be completely suppressed resulting in a single mode emission with high coherence length. During the warm up of the laser tube the modes are sweeping while changing their intensity due to the Doppler broadened gain profile (Fig. 2.23). By recording a range of oscilloscope tracks the gain profile can be determined as well. Even without using the PZT some important static patterns of the Fabry Perot can be recorded. In this case the translucent screen is used and with a digital camera the created patterns are photographed. In this way the transversal modes of the Fabry Perot are taken and the surface quality of the spherical mirrors evaluated.

Measurements with the HeNe Laser

The extension kit comes with a two mode HeNe-laser (2) which is mounted into the two XY fine adjustment holder (4). Soft silicon rubber O-rings keep the HeNe-laser tube in position allowing beside the XY translation also a tumbling motion. The necessary high voltage for the operation of the HeNe-laser is provided by the power supply (1). Due to the larger dimensions of the HeNe-laser a 1000 mm long optical rail (5) is provided. For the demonstration of the linear and orthogonal polarised modes a polarizer and a holder with a scale is provided All other components are the same as used within the LM-0300 Fabry Perot experiment (44). The mirrors are coated for 532 nm as well as for 632 nm thus there is no need for extra mirror to operate the Fabry Perot with the red line of the HeNe-Laser. Once aligned, a mode spectrum as shown in Fig. 2.24 is obtained. The spectrum has been taken with the 75 mm mirror set. Consequently the free spectral range (FSR) is 1 GHz. A pair of modes appear and depending on the warm-up state of the laser tube these modes are wander and change their amplitude. Two different mode spacings Δν can be identified:

$$\Delta\nu_1 = 295 \text{ MHz and } \Delta\nu_2 = 729 \text{ MHz}$$

At this point it becomes clear that a Fabry Perot cannot measure absolute values and one has to know something more about the probe laser. The HeNe-laser has a Doppler broadened profile with a gain width of 1.5 GHz (Fig. 2.23). With the Fabry Perot we observe only two modes. If we assume the mode spacing $\Delta\nu_1$ is the correct one, then we have to expect 5 modes (1.5 GHz / 0.295) which obviously is a contradiction to the measurement. Actually $\Delta\nu_2$ is the correct value, indeed the manufacturer specifies 730 MHz.

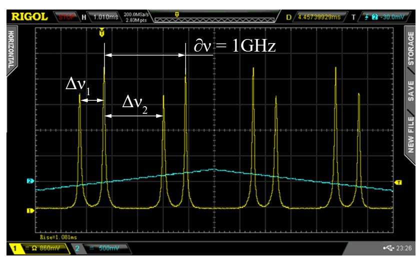

Fig. 2.24: Spectrum for 75 mm mirror

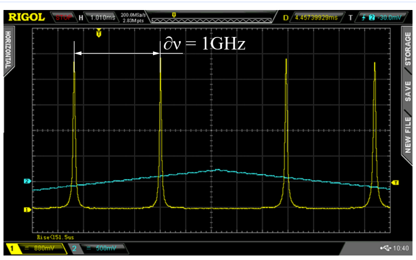

Fig. 2.25: Mode suppressing with a polarizer

Since the two modes are orthogonally polarized a polarizer in front of the HeNe-laser blanks one mode. Fig. 2.26 shows the spectrum of the HeNe-laser with a flat mirror FP. To achieve a passable finesse the use of the beam expander is required.

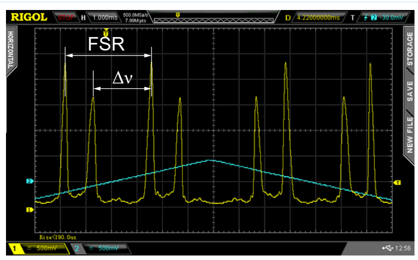

Fig. 2.26: Mode spectrum with flat mirror and expanded probe laser beam

Some other interesting measurements can be performed using the static Fabry Perot. Picture A in Fig. 2.27 appears for the Fabry Perot adjusted to the confocal distance. Dark zones are originating from deviation of the mirror from a perfect sphere.

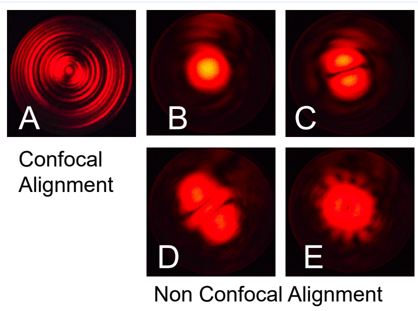

Fig. 2.27: Static mode pattern

Figures B, C, D and E are showing the transverse modes of the non confocal adjusted Fabry Perot. In B the fundamental mode TEM_{00} and in E the so called doughnut mode is visible.

LM-0330 Two Mode HeNe Laser Extension Kit consisting of:

Item	*Code*	*Qty.*	*Description*	*Details page*
1	DC-0062	1	High voltage supply 5 mA	122 (8)
2	LQ-0300	1	Two mode HeNe laser Ø30 housing, 632 nm	120 (14)
3	MM-0024	1	Mounting plate C25-S on carrier MG20	93 (2)
4	MM-0470	2	XY mount, soft ring 30 mm, on MG20	97 (32)
5	MP-0100	1	Optical Bench MG-65, 1000 mm	92 (4)
6	OC-0710	1	Polarizer in C25 mount	102 (34)

Highlights

Premium class ★★★ experiment
Stable two mode HeNe-laser
Demonstration of transverse modes

LM-0400 Laser Range Finder

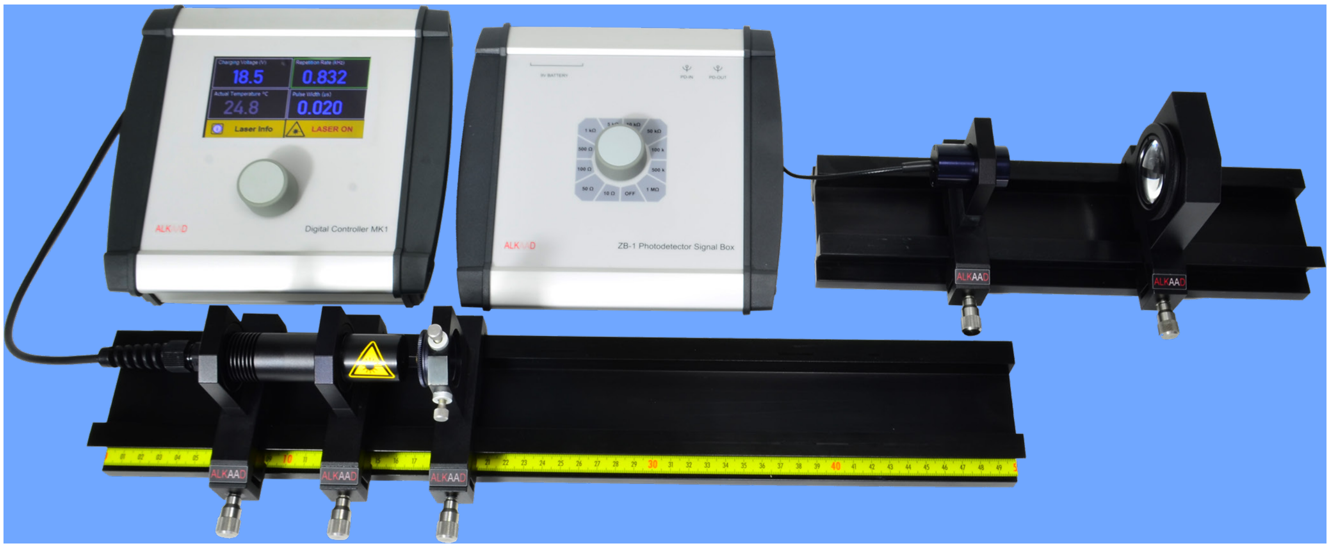

Keywords

Short pulse laser diode
Beam Collimator
Time of Flight
Peak Power
Fast Si PIN Photodetector
LIDAR
Laser Energy
Light Echoes

Introduction

Laser range finding is one of the applications of light detection and ranging known as LIDAR. The principle of this technique is well known from the RADAR (Radio wave Detection And Ranging). Instead of using radio waves, the LIDAR uses light as electromagnetic wave. Both techniques are based on the emission of a short pulse of electromagnetic radiation and the reception of back scattered signals from a target. The time t between the emission and reception of the pulse is measured and the distance d is calculated based on the velocity v of electromagnetic radiation. Using $v \approx 3 \times 10^8$ m/s for the speed of light, the time interval t for a distance d of 10 m will be 66 ns. The pulse duration must be modified to match the required resolution and distance. In this experiment the shortest pulse duration is 50 ns with a rise time of 5 ns. When the laser pulse is launched, the receiver photo detector is also used to generate a start pulse signal which serves as trigger for the oscilloscope. The peak power of the laser diode amounts to 70 W within 100 ns which is related to an energy of 4 µJ only. The intensity of the back scattered light is very low compared to the laser pulse itself and depends on the scatter efficiency of the target. Furthermore the intensity drops with $1/r^2$ where r is the distance to the target. Consequently a photodetector with amplifier is used. The controller allows also the characterization of the laser diode itself. The output power and pulse width as function of the parameters like charge voltage and discharge time can be measured and optimised for the length to be measured.

How it works

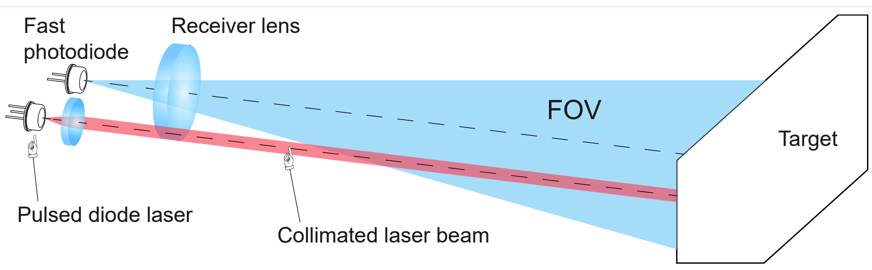

The emission of the pulsed diode laser is collimated to an almost parallel laser beam. At a certain distance it hits the target from which scattered light travels back depending on the scatter properties of the target. The receiver lens captures according to its field of view (FOV) a small fraction of it and focuses it onto a fast photodiode. Because only a small fraction of the incident light comes back, a fast and sensitive amplifier is needed.

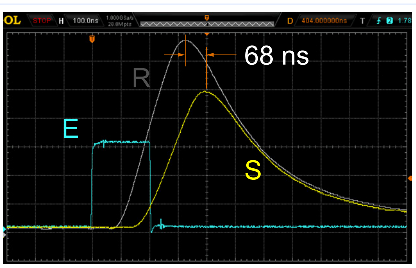

Fig. 2.28: Measurement of the time of flight

For the operation of the laser range finder an oscilloscope is required. The Fig. 2.28 shows the principle of a measurement with target which is 10 m apart. The blue trace (E) shows the electrical pulse for the diode laser. To get the optical laser pulse at zero distance a target (sheet of A4 paper for instance) is held in front of the setup and the resulting curve is stored on the scope as reference curve (R). After removing the target at the zero position the new curve is stored as well. At the peak of the reference the time is defined as zero and the distance to the next peak gives the time of flight t for one round trip.

$$2 \cdot s = v \cdot t$$

According to this, the travelled distance s is:

$$s = \frac{1}{2} v \cdot t$$

whereby *v* is the speed of light. If the distance is known we can also determine the speed of light.

LM-0400 Laser Range Finder consisting of:

Item	*Code*	*Qty.*	*Description*	*Details page*
1	CA-0060	1	Infrared display card 0.8 -1.4 µm	127 (10)
2	CA-0450	2	BNC connection cable 1 m	130 (28)
3	DC-0050	1	Pulsed laser diode controller MK1	122 (6)
4	DC-0220	1	SiPIN Photodetector, ultrafast with amplifier	124 (23)
5	MP-0130	2	Optical Bench MG-65, 300 mm	93 (7)
6	OM-0520	1	Pulsed diode laser head in twofold rotary mount	113 (22)
7	OM-0620	1	Collimating optics on carrier MG20	114 (30)
8	OM-0622	1	Focussing optics, f=60 mm on carrier MG20	115 (31)
9	UM-LM04	1	Manual Laser range finder	
	Required Option (order separately)			
10	CA-0200	1	Oscilloscope 100 MHz digital, two channel	129 (19)

LM-0500 Laser Doppler Anemometer (LDA)

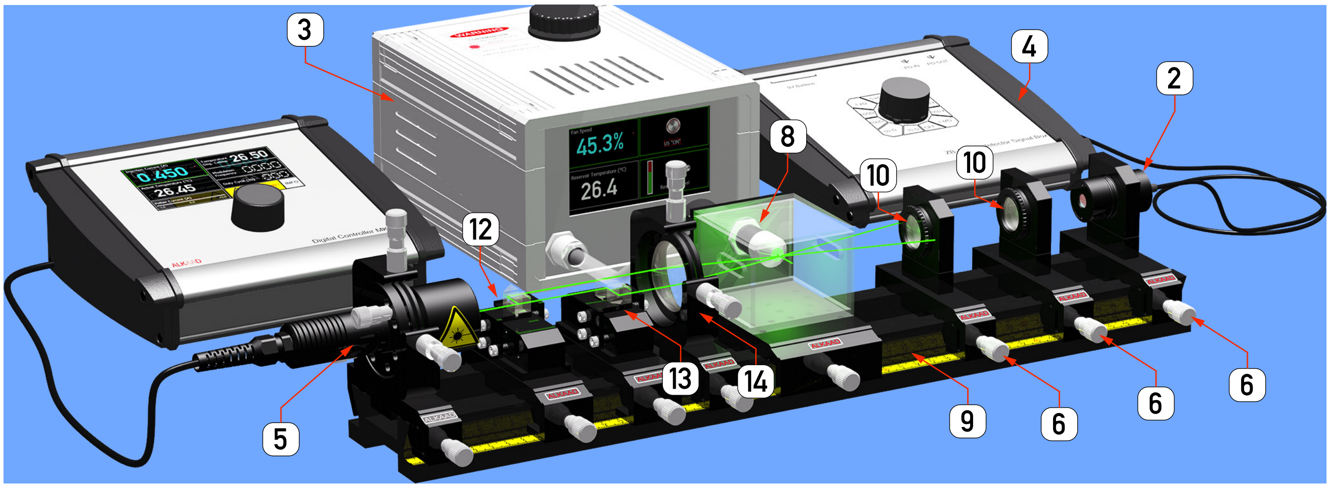

Dual Beam Interference
Light Scattering
Ultrasound Particles Generator
Spatial Interference
Measuring Particle Speed
Fourier Transformation
Doppler Effect
Spatial Scattering

When children play while striking the vertical bars of a picket fence with a stick it gives a characteristic burst like noise. The faster they are running the shorter the burst is, however the frequency of the strikes is higher. The same principle Yeh and Cummins exploited 1964 when they invented their Laser Doppler Anemometer. Anemos is a Greek word and means "wind", consequently a Laser Doppler Anemometer (LDA) can be considered as a "wind meter" using a laser. However the LDA cannot detect pure wind as a clean air stream, it needs to have particles moving with the wind, These particles are guided to move through two crossing laser beams created from one source.

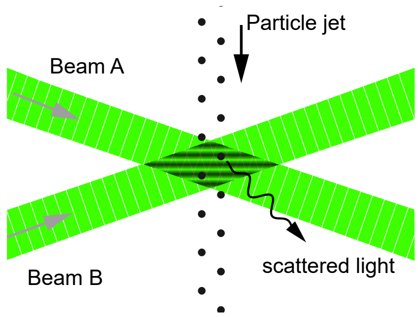

Fig. 2.29: Beam crossing zone

Due to the coherence of the laser and thus also of the two beams a spatial interference pattern appears within the crossing zone looking like zebra stripes. When particles are moving through the stripes they scatter the light in preferred directions. The set-up uses an ultra sonic particle generator. "Dry" water particles ejected through a nozzle perpendicular cross the interference zone. A photodetector combined with a fast and sensitive amplifier is used to detect the scattered light. A storage oscilloscope is required to display and store the individual burst for the subsequent analysis. Modern oscilloscopes are provided with an in-built fast Fourier analyser for real time display of the burst frequency.

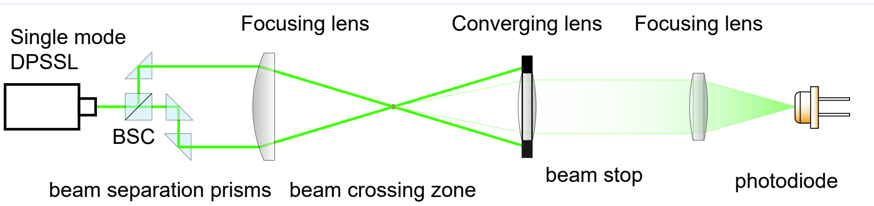

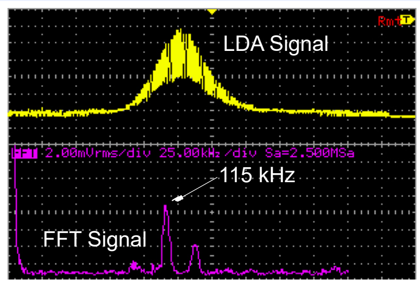

Fig. 2.30: Oscilloscope screen dump

Special care must be taken in the selection of the laser source as well as the beam splitting section. Both components contribute significantly to the contrast of the interference fringes in the beam crossing zone. The laser source should be a single mode laser with a Gaussian beam profile in TEM_{00} mode. Furthermore the polarisation of beam A and B must be the same which requires a careful selection of the beam splitting and bending prism. Another design criteria is the aberration minimized imaging of the focusing lens. Finally the beam stop and the photodiode sensitivity with subsequent amplifier determine a good signal to noise ratio.

Another key is the provision of a suitable particle jet consisting of small and "dry" particles. The experiment comes with a two stage ultrasound particle generator with adjustable jet flow speed. The Fig. 2.30 shows a burst event with simultaneous FFT. It will take a while to catch such events since a lot more events exist. It is important to set the trigger of the oscilloscope to single events with a trigger level high enough not to react on small bursts. Also one trace will contain probably more than one burst, but a digital oscilloscope can be focused and expanded to a desired event. The storage possibility of the oscilloscope allows also storing of the data on a USB stick for further evaluation with Excel or other software.

LM-0500 LDA - Laser Doppler Anemometer consisting of:

Item	*Code*	*Qty.*	*Description*	*Details page*
1	CA-0012	1	Set of tools for LDA	126 (3)
2	DC-0220	1	SiPIN Photodetector, ultrafast with amplifier	124 (23)
3	DC-0320	1	US particle generator	125 (28)
4	DC-0380	1	Photodetector Junction Box ZB1	125 (31)
5	LQ-0040	1	Green (532 nm) stabilized Laser, 40 mW	119 (3)
6	MM-0020	3	Mounting plate C25 on carrier MG20	93 (1)
7	MM-0060	1	Filter plate holder on MG20	94 (7)
8	MM-0800	1	Adjustable fog nozzle on MG30	98 (42)
9	MP-0150	1	Optical Bench MG-65, 500 mm	93 (8)
10	OC-0060	2	Biconvex lens f=60 mm in C25 mount	99 (5)
11	OC-0420	1	LDA alignment aid	100 (20)
12	OM-0060	1	LDA Beam splitter unit	111 (6)
13	OM-0062	1	LDA Beam Displacer	111 (7)
14	OM-0066	1	LDA beam focussing unit	111 (8)
	Required Option (order separately)			
15	CA-0200	1	Oscilloscope 100 MHz digital, two channel	129 (19)

LM-0600 Laser Gyroscope

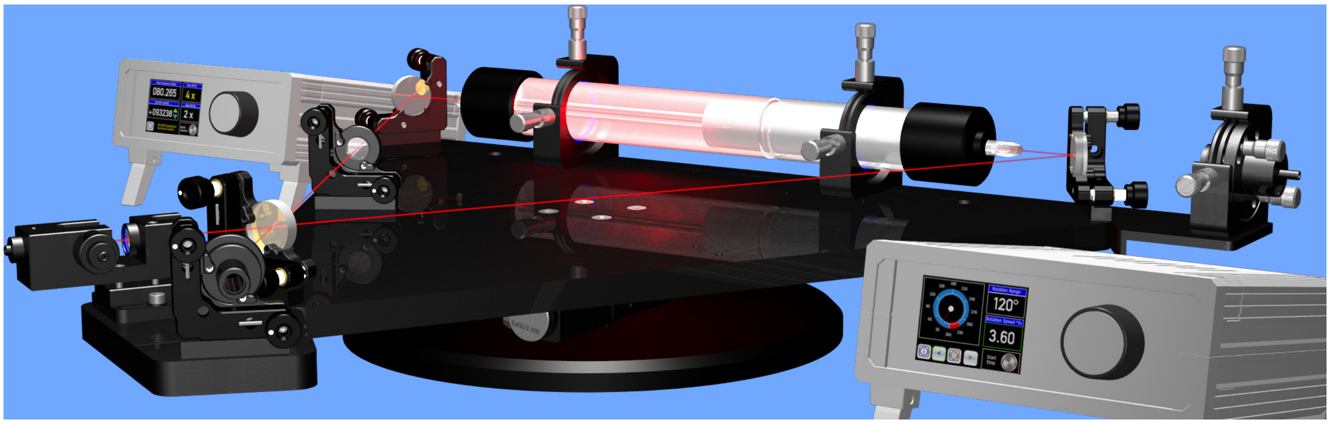

Keywords

Sagnac Effect	**Interference**	**Half and quarter wave plates**
HeNe Ring Laser	**Beat Frequency Detection**	**Optical 90° phase shifter**
Single Mode Etalon	**Linear and Elliptical Polarisation**	**Direction Discrimination**
Lock-In Effect	**High Precision Angle Measurement**	**Active Laser Gyroscope**
Processor Controlled Rotation	**Quad Frequency Counting**	

Introduction

Despite the existence of high precision satellite navigation (GPS) each transport vehicle which relies on navigation must have its own GPS independent navigation system to be prepared if the GPS may fail. Regardless of the manufacturer like Airbus or Boeing, air planes nowadays are equipped with laser gyros for navigation.
Shortly after the invention of the laser in 1960 the idea of Georges Sagnac from 1913 (France) was applied in conjunction with a HeNe ring laser. However the difference of such a ring laser gyroscope to the idea of Sagnac lies in the fact that within Sagnac's set-up the light source is separate from the ring structure and the signal is as a phase shift between the counter propagating beams. In the laser gyroscope discussed and applied here, the light source is part of the ring laser and the output is a beat frequency between the counter propagating laser modes. This class of laser gyroscopes are termed as "active" and those of the Sagnac' s type as "passive" laser gyroscopes. In general the active laser gyroscope provides a much higher precision and long term stability as against the passive ones. The basic specifications are:

Range:	$1x10^{-6}$ to $1x10^{3}$ °/sec
Resolution:	app. 2 arc sec
Zero stability:	$1x10^{-3}$ °/h
Scale factor stability:	app. 3 ppm

The precision of the laser gyro becomes more evident, when it is compared to other well known measuring devices for instance a micrometer screw gauge with a resolution of 0.01 mm. It must have at least a length of at least 3 km (!) for having the same resolution.
Within this experimental system the basics of the laser gyro are explained and practically studied at the system, which allows full access to all components. The experimental laser gyroscope consists of a rugged turntable on which the ring laser is mounted. A rotational stage driven by a stepper motor rotates the turntable. The angular speed and range can be set via the provided controller. The ring laser consists of three laser mirrors arranged at the corners of an equilateral triangle. The point of rotation lies well within the centre of this triangle. At one mirror a beam bending device is positioned in such a way that the clockwise and counter clockwise propagating modes are superimposed and the beat frequency is detected by two photo detectors. The signal of the photodetector has a phase shift of 90° to each other so that a subsequent direction discrimination is performed. The created TTL signal is fed to a frequency counter.
For the first alignment of the ring laser an adjustable green laser pointer is used. Once the system is aligned, the single mode etalon is inserted to obtain the required single mode operation. The beat frequency of the modes is measured as function of the angular speed. A special measurement is focused on the so called lock-in threshold, which is an unwanted effect of active laser gyroscopes.

How it works

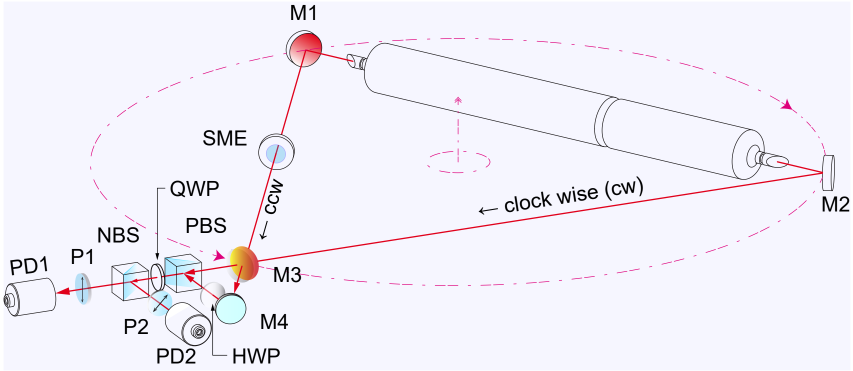

Fig. 2.31: Principle of Helium Neon Laser Gyroscope

At the mirror M3 a fraction of both the cw and ccw mode leaves the ring cavity formed by the three mirror M1, M2 and M3. Both modes are linearly polarised whereby the polarisation direction is defined by the Brewster windows attached to the laser tube. The cw beam enters and directly leaves the polarising beam splitter (PBS). The ccw beam is directed in such a way that its direction is perpendicular to the cw beam. The half wave plate (HWP) turns the polarisation direction of the ccw beam by 90° thus the beam is reflected at the PBS and travels from here onwards collinear to the cw beam which is necessary for the superimposition to obtain the beat frequency. After leaving the PBS both beams are travelling in one direction however, the polarisation state is orthogonal to each other. The quarter wave plate (QWP) converts both beams into circular polarisation, one right and the other left circularly oriented. If both modes having the same frequency the respective electrical field vector are rotating with the frequency ω the resulting vector is fixed in its orientation. As soon as there is a frequency shift between the two modes, the resulting vector starts to rotate with the beat frequency of $\omega_b=\omega_{cw} - \omega_{ccw}$.

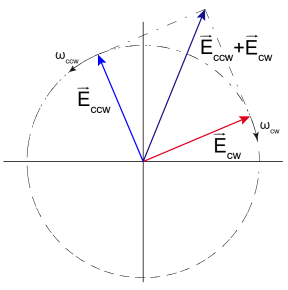

Fig. 2.32: Vectorial presentation of the electrical field vector of the cw and ccw mode.

By placing photodetector behind a polarizer (P1) the rotating E vector is converted into a corresponding intensity variation. The neutral beam splitter (NBS) divides the two circular polarised beams into two channels each having a photodetector (PD1, PD2). The polarizer P2 in front of the photodetector PD2 is tilted by 45° with respect to P1 resulting in a 90° phase shift between the signal of PD and PD2 which will be used in a phase discriminator to detect whether the gyroscope rotates cw or ccw.

Description of the components

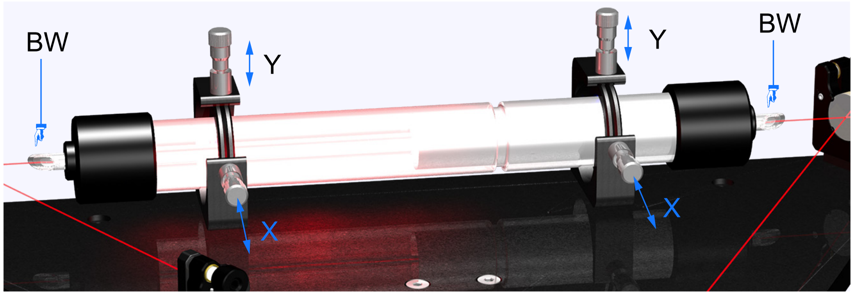

Fig. 2.33: **Helium Neon Laser Tube**

The Helium Neon laser tube is terminated with two Breswter windows (BW) and is mounted into a pair of XY adjusters (XY). The tube is fixed by slightly pressed soft rubber O-rings. The precise adjustment screws allow the tube to be aligned in XY direction. The interplay of both adjusters also allows the angular wobble of the tube. For the operation, a high voltage power supply is supplied (DC-0064) which provides the start-up ignition voltage of about 10 kV and 6.5 mA at 1400 V for the continuous operation.

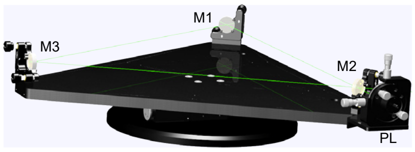

Fig. 34: Laser Ring Cavity

The sturdy and yet light weight ribbed aluminium plate has an equilateral shape. On each corner an adjustable laser mirror holder is mounted forming with mirror M1, M2 and M3 the optical cavity. The plate is attached to the drive unit by means of four countersink screws and will be dismounted from the drive unit before shipment. Although it is not really a circle such a cavity is also termed as ring cavity. The distance between the mirror is 460 mm resulting in a cavity length L of 1380 mm and free spectral range (δν=c/L) of 217 MHz.

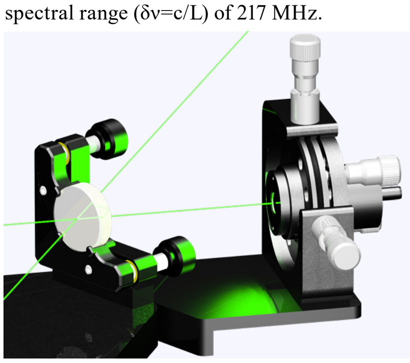

Fig. 35: Green adjustment laser

For the reliable alignment of the mirror of the laser ring cavity, a green emitting laser pointer is used. It is held in a four axes adjustment holder in such a way that the pilot laser can be shifted and tilted to align the alignment beam with respect to the laser tube via the mirror M2.

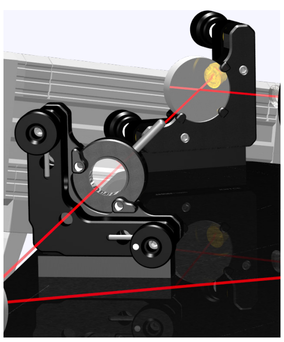

Fig. 36: Single mode etalon

For the operation of the laser gyroscope it is required that the laser operates in a single mode only. This is achieved by inserting an etalon into the cavity. A kinematic adjustment holder allows the precise orientation of the etalon with respect to the laser beam.

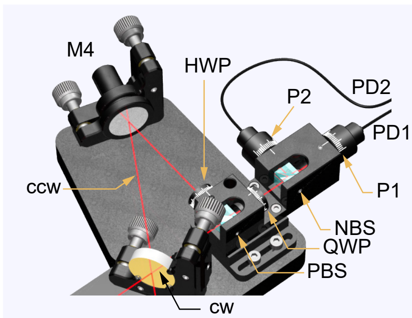

Fig. 37: Dual beat frequency detector

To obtain the beat frequency, the cw (clockwise) and the ccw (counterclockwise) modes must propagate collinearly. At mirror M3 a small fraction of both modes is leaving the cavity. The cw mode passes directly the polarising beam splitter (PBS) and the ccw mode is reflected by the mirror M4 in such a way that it enters the polarising beam splitter (PBS). Since it has the same polarisation as the ccw mode we need to turn its polarisation by 90° so that the mode is reflected inside the PBS and continues to travel collinear with the cw mode. Now both modes are perpendicularly polarised to each other. The quarter waveplate (QWP) converts both modes into circular polarised light. By using a neutral beam splitter (NBS) with a splitting ratio of 1:1 we create two channels. At the end of each channel a polarizer (P1, P2) is located in front of a photodetector (PD1, PD2) converting the light back to linear polarisation allowing the detection of the beat frequency. To obtain a 90° phase shifted optical signal the polarizer P1 and P2 are oriented under an angle of 45° to each other. This allows the detection of the rotation direction of the laser gyro. The photodiodes PD1 and PD2 are connected to the 2 channel photodiode amplifier DC-0080.

Fig. 38: DC-0080 Quad counter & 2 channel photodiode amplifier

The microprocessor controlled amplifier DC-0080 contains two independent amplifier channels whereby the gain of each can be set via the touch screen and the one knob digital selector. The amplified photodetector signals are internally converted to TTL signals and fed to the internal quadrature counter. The microprocessor reads and transfers the counter results to the display as numerical value of the frequency, the counted fringes and the direction of rotation. The analog as well as TTL signals of the photodetector channel are available at the rear panel via BNC sockets. Due to the quadrature signals an interpolation can be performed which results in a maximum 16 times higher resolution.

Fig. 39: Turntable drive unit

The turntable is rotated by a stepper motor which drives a zero-play pre-loaded worm gear drive. The powerful stepper motor needs 200 full steps per turn which relates to a rotation of 2° or 0.6' per step. The stepper motor is connected via a 15 pin Sub-D connector to the DC-0300 stepper motor controller.

Fig. 40: DC-0300 Stepper motor controller

The microprocessor controlled DC-0300 operates the turntable drive. It can drive the stepper motor in full step or micro step with 1/2 to 1/16 micro steps. By means of the touch panel and the one knob digital selector, the speed can be set in a range from 0.1 to 12 °/s and the maximum rotation range of ±180°. The controller can repeat the rotation by an adjustable number of repetitions. The provided remote control is a useful add-on for the initial alignment or demonstration to an audience.

Both the controller, the DC-0080 quad counter and photodiode amplifier and the DC-0300 Stepper motor controller are equipped with a USB bus and can be controlled by the Laser gyroscope control software WIN in combination with an external PC or tablet.

The LMH-0600 Laser gyroscope can be fully operated without any external computer.

Experimental Work

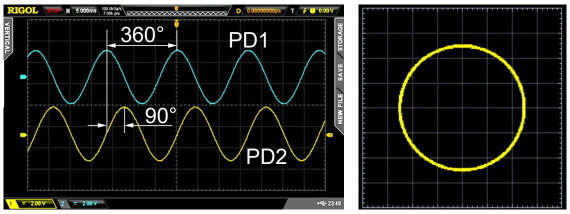

Fig. 2.41: Beat frequency signals 90° phase shift and XY representation

Once the initial alignment of the ring cavity has been completed and the ring laser operates with the inserted etalon, it is time to adjust the beat frequency detector. PD1 and PD2 are connected to the photodiode amplifier and the output connected to an oscilloscope. By aligning the polarizer P1 and P2 the phase shift of 90° between the signal of PD1 and PD2 is achieved. In case both amplitudes are the same a circle appears when the oscilloscope is switched to the XY mode. If the gyroscope is resting, only a dot on the circumference track is visible. Depending of the rotation direction, this dot moves accordingly.

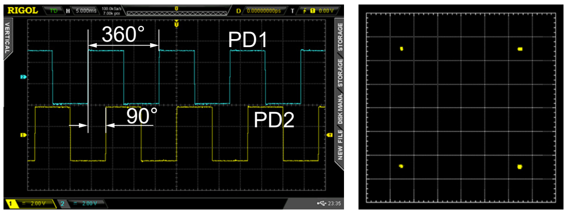

Fig. 2.42: Beat frequency converted to TTL and its XY representation

The DC-0080 amplifies not only the photodiode signal, it also converts it to TTL level. In the XY representation we will notice a dot jumping from one corner to the next one. Depending on the rotation of the laser gyro this dot either jumps in cw or ccw direction. The TTL signal of PD1 and PD2 is connected to the input of a quadrature counter which fulfils three tasks. Firstly it interprets the rotation direction, secondly it counts the TTL events and thirdly it can interpolate one event into 4 (each dot of the corner). In frequency mode the beat frequency is measured and displayed.

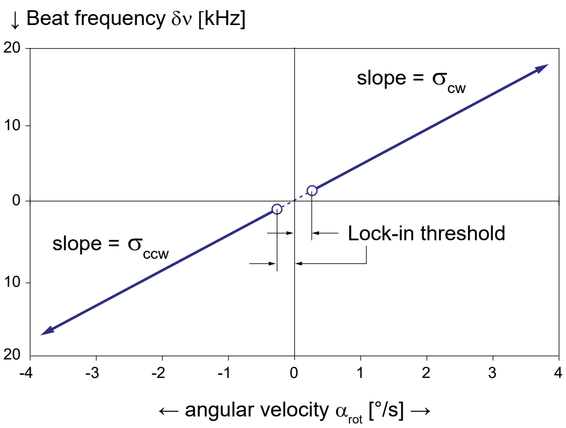

Fig. 2.43: Lock-in threshold and gyro constant

$$\delta\nu_{beat} = \frac{4 \cdot F}{L \cdot \lambda} \cdot \omega_{rot}$$

This formula derived from Sagnac's equations describes the dependency of the beat frequency on the rotary frequency ω_{rot} and constant parameter of the gyroscope. F denotes the area which is encompassed by the light beam, L is its circumference and λ the wavelength of the laser. Applying this formula to our gyroscope with the equilateral shape with the length a of one side of 460 mm we get

$$\delta\nu_{beat} = 4.202 \cdot 10^5 \cdot \omega_{rot}$$

Converting ω_{ro} into the angular velocity α_{rot} in °/s we get:

$$\delta\nu_{beat} = 7.334 \cdot 10^3 \cdot \alpha_{rot}$$

With an angular speed of 1°/s for example, we should expect a beat frequency of 7.334 kHz.
It is a part of the measurement task to determine this value. The stepper motor controller is set in such a way that the gyro shall turn let's say 180 ° in cw and subsequently in ccw direction for a given set of angular velocities α_{rot}.
A sample graph with arbitrary units is shown in Fig. 2.43. From the slope of the cw and ccw rotation we will get the value of σ and compare it with the predicted value. Furthermore the lock-in threshold is determined.

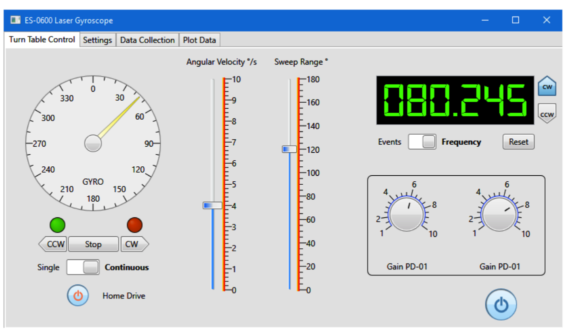

Fig. 2.44: Laser gyroscope control software WIN

You may want to perform automated measurement or demonstrate the experiment as a live lecture in front of your students. In this scenario the "Laser gyroscope Control software WIN" is the right choice. From a central location like a notebook for instance, the entire experiment can be controlled and automated measurements taken. In case the laptop is connected to the video system of the lecture hall the students can see the experiments via the lecture hall camera and the control and incoming data via the notebook on the lecture hall screen. To operate the software both controller the DC-0080 as well as the DC-0300 are connected via their USB busses to the notebook. All required settings like the angular velocity, rotation range and direction are accessible. Furthermore the gain of the photodiode amplifier and the settings of the quadrature and beat frequency counter can be set by the software.
A central feature is the automated operation and data collection possibility. The laser gyroscope is operated at different rotation velocities and direction whereby the beat frequency is recorded. A live graph is displayed and can be printed or stored either numerical or graphical form as PDF document.

LM-0600 HeNe Laser Gyroscope consisting of:

Item	Code	Qty.	Description	Details page
1	CA-0080	1	Optics cleaning set	128 (12)
2	DC-0064	1	High voltage supply 6.5 mA	122 (9)
3	DC-0080	1	Quad counter & 2 channel photodiode amplifier	123 (11)
4	DC-0100	1	Stepper motor controller	123 (13)
5	MM-0700	1	Turntable drive unit	98 (41)
6	OM-0700	1	Gyroscope turntable	116 (39)
7	OM-0720	1	Alignment laser 532 nm with power supply	116 (40)
8	OM-0780	1	Dual beat frequency detector	116 (41)
9	UM-LM06	1	Manual HeNe laser gyroscope	
	Option (order separately)			
10	ES-0600	1	Laser gyroscope control software WIN	
	Required Option (order separately)			
11	CA-0200	1	Oscilloscope 100 MHz digital, two channel	129 (19)

Highlights

Premium class ★★★ experiment
★ No external computer required
★ New directional discrimination

Intended institutions and users:
Advanced
Physics Laboratory
Engineering department
Electronic department
Naval college, aerospace, aviator and earth-bound navigation

LM-0700 Laser Safety

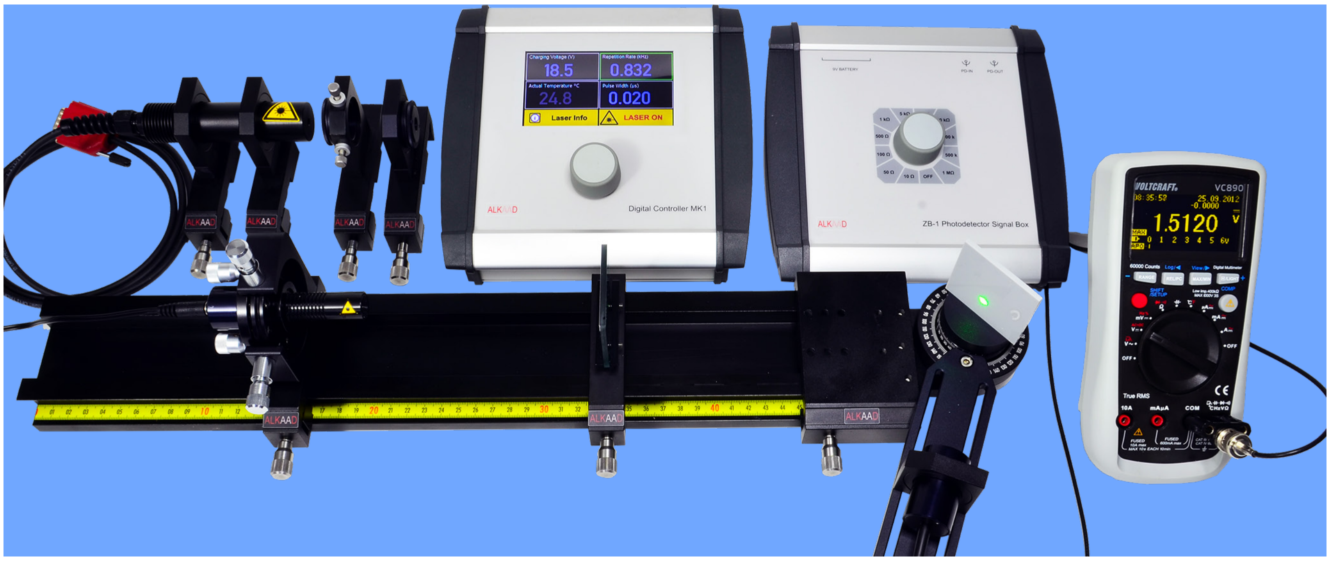

Laser Application

Keywords

IEC 60825 or ANSI Z136
Laser Intensity
Damaging Effects
Pulsed Laser
Laser Safety Regulations
Max. Permissible Radiation
Laser Classification
Laser Beam Divergence
Safety Distance
Safety Goggles

Introduction

In this experiment the students are encouraged to convert the essential theoretical contents regarding „Laser Safety“ into practice. The application and use of the basics in calculation defined within the standards is submitted and trained by practical examples. The major measurement task is to determine the intensity of a laser beam which is defined as power per cross section typically given in W/m². The power is measured by using a calibrated power meter. The cross section and the divergence is determined by a set of imaging lenses with known focal lengths. In addition to the direct exposure also the danger of scattered light is classified by using a scatter probe mounted on a pivot arm.
The experiment is divided into of several segments. Aspects such as the following ones have been considered:

1. Determination of the maximum permissible radiation (MPR) for skin and eyes
2. Minimum safety distance from a radiation source for direct and indirect irradiation of the skin and the eyes, (MSD)
3. Characterization of a pulsed laser systems
4. Requirements for laser safety goggles, transmission of optical filter

The fundamentals of IEC 60825 or ANSI Z136 or corresponding literature of laser safety should be known. The danger of lasers are understood by the characteristic properties of the laser radiation. In comparison with other light sources, a high energy and power density can be attained, because of the generally small beam divergence the radiation density can be very high even at large distances from the laser (potential danger of lasers used in metrology).

Not only the direct radiation also reflected and scattered radiation can cause damage at a large distance from the radiation source. Laser radiation can be generated within a broad spectral range. It extends from a few nanometre up to some hundred micrometers and is, in many cases, outside of the visible spectrum.
The damage of the biological tissue (skin, eye) depends strongly on the wavelength and on the duration of the exposure. This is of great importance under safety aspects when classifying the lasers and fixing radiation limits which is also subject of this experiment. By means of two different laser sources all parameters are measured in order to classify each laser and to determine the limits for which the laser can be considered as safe. This includes also the characterization of laser safety goggles.

How it works

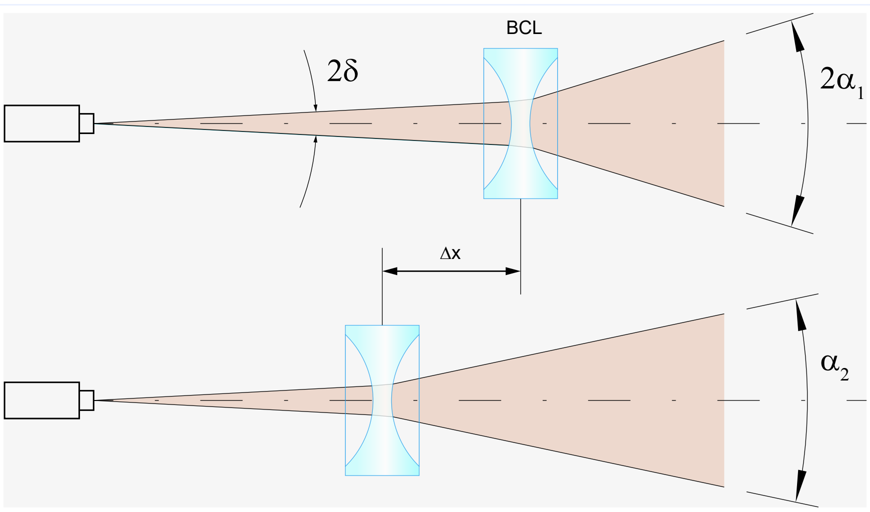

An easy way to measure the important value of the divergence of the laser beam is to measure the enlarged diameter of the laser on a distant wall. However, this is not suitable in all cases. Thus we have introduced a diverging lens (BCL) to simulate the same effect. By using the goniometer the divergence angle is measured for a known distance from the laser. Applying the ABCD matrix formalism with the known transfer matrix [T] of the diverging lens (BCL) and related data and distances the unknown angle δ is determined:

$$\begin{pmatrix} T_1 & T_2 \\ T_3 & T_4 \end{pmatrix} \cdot \begin{pmatrix} r_1 \\ \delta \end{pmatrix} = \begin{pmatrix} r_2 \\ \alpha_2 \end{pmatrix}$$

In a more refined way the laser divergence is determined by carrying two or more measurements.

Description of the components

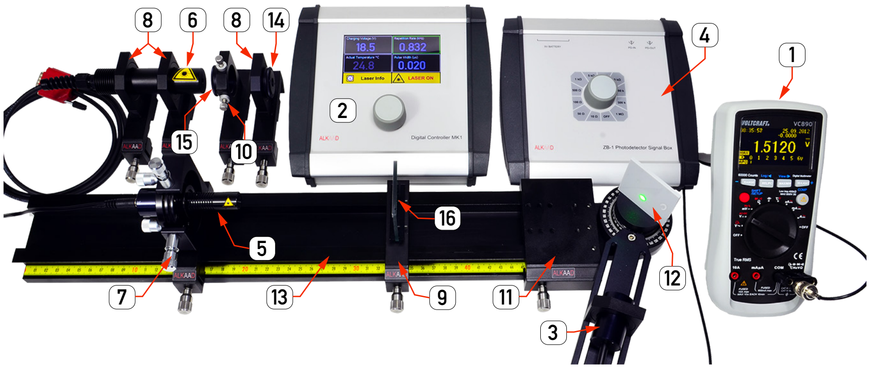

The experiment comes with two laser sources. One is a green emitting DPSSL (5) with an output power of 5 mW and the other is a pulsed diode laser with an output energy of 4 µJ. The green laser is operated with a wall plug power supply, whereby the pulsed laser (6) is powered by the digital controller (2). For the collimation of the divergent radiation of the pulsed diode laser a collimator (15) is provided, which is used in conjunction with the precision XY adjustment holder (19). The green laser is mounted into a 4 axes adjustment holder (7) by which the direction of the laser radiation is aligned with respect to the optical axes of the optical bench. The goniometer (11) is attached to the optical bench (13) and allows to measure the angle resolved emission of a laser source. The laser power is detected by a photodetector (3) which is attached to the rotary arm. The photodetector is connected to the junction box (4) where the detected photocurrent is converted into a voltage and displayed on the digital voltmeter (1). Furthermore, a filter (16) is provided. Its transmission is measured by using both laser sources and determined for which laser the filter is a suitable safety goggle material.

Measurements

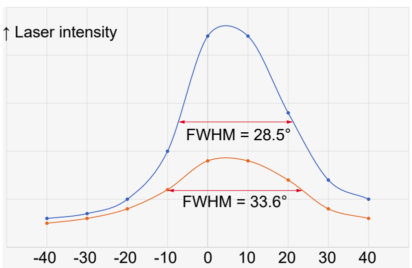

Fig. 2.45: Measurement of the divergence

To determine the maximum permissible radiation (MPR) the laser safety officer needs to know the wavelength, the beam diameter, laser power and finally the mode of operation, if pulsed or continuous mode. To get the MPR from the tables of the laser safety regulations one needs to know the laser intensity in W/m². The continuous laser power in watt or milliwatt is measured by a calibrated power meter (like 19,21). Dividing the measured value by the beam cross section we get the intensity. In order to determine the MPR in a defined distance, the officer needs to know in addition the divergence of the laser. Due to the large divergence of the pulsed laser it can be measured straight forward by using the goniometer. For the green laser with a much smaller divergence this method fails. That is why we need to increase the divergence first by using a lense (14) with known parameter. By using the ABCD parameter, the divergence of the laser source can be calculated backwards based on the measured divergence behind the lens. Such a measurement example is shown in Fig. 2.45.

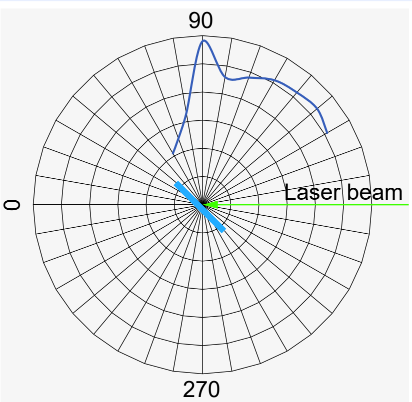

Fig. 2.46: Scattered intensity versus emission angle

The previous considerations targeted the safety of the human eye. In this section the irradiation of the human skin by scattered laser light is treated. Wearing laser safety goggles only protects the eyes, but what is about the scattered light from surfaces hit by the laser beam. To study this phenomenon a scattering surface is placed into the centre of the goniometer and illuminated by the green laser beam. The scattering surface is oriented under 45° with respect to the incident laser beam (see Fig. 2.46). The photodetector is turned around the probe and lets say for each 5 or 10 ° the value detected by the photodetector is taken. It makes sense to transfer the values into a chart with polar coordinates (Fig. 2.46). The curve shows a peak at 90° which indicates that the surface has also a slight directed reflectivity compared to a standard cosine scattering material. The absolute scattered power can be measured using the calibrated instrument (19, 21) or the provided photodetector. As already mentioned the junction box converts the photocurrent I_p into a voltage by measuring the voltage drop across the series resistor of the photodiode. This resistor R can be set via the knob on the front panel and the supply voltage is 9 VDC. From the voltage drop, the known resistor R and voltage we can determine the photocurrent. From the provided spectral sensitivity curve of the used photodiode we calculate the incident power.

LM-0700 Laser safety consisting of:

Item	*Code*	*Qty.*	*Description*	*Details page*
1	CA-0220	1	Multimeter 3 1/2 digits	129 (21)
2	DC-0050	1	Pulsed laser diode controller MK1	122 (10)
3	DC-0120	1	Si-PIN Photodetector, BPX61 with connection leads	123 (15)
4	DC-0380	1	Photodetector Junction Box ZB1	125 (31)
5	LQ-0020	1	Green (532 nm) DPSSL in ø25 housing	119 (1)
6	LQ-0350	1	Pulsed diode laser in housing	120 (15)
7	MM-0420	1	4 axes adjustment holder	96 (25)
8	MM-0020	3	Mounting plate C25 on carrier MG20	93 (1)
9	MM-0060	1	Filter plate holder on MG20	94 (7)
10	MM-0090	1	XY adjuster on MG20	94 (8)
11	MM-0300	1	Carrier with 360° rotary arm	95 (20)
12	MM-0340	1	Scatter probe on rotary table	95 (21)
13	MP-0150	1	Optical Bench MG-65, 500 mm	93 (8)
14	OC-0010	1	Biconcave lens f=-10 mm, C25 mount	98 (2)
15	OC-0170	1	Collimator 808 nm in C25 mount	99 (13)
16	OC-0939	1	Filter BG39, 50 x 50 x 3 mm	104 (53)
17	UM-LM07	1	Manual Laser Safety	
	Option (order separately)			
18	CA-0200	1	Oscilloscope 100 MHz digital, two channel	129 (19)
19	CA-0260	1	Laser power meter LabMax-TO	129 (22)
20	CA-0262	1	Energy sensor head 300 nJ - 600 µJ	129 (23)
21	CA-0264	1	Power sensor LM2 VIS 50 mW / 1 nW	129 (24)

Highlights

Premium class ★★ experiment

Intended institutions and users:

Laser safety officers
Physics Laboratory
Engineering department
Electronic department

LM-0800 Barcode Reader

Types of Barcodes
Scanning Algorithm
Photodetector
Visible Diode Laser
Barcode Detection
Computer Integration
Rotating Polygon Mirror
Barcode Recognition

The development of the barcode reader principle goes back to 1948 when Bernard Silver, a graduate student at Drexel Institute of Technology in Philadelphia overheard a conversation between the president of the local food chain and one of the deans. The president asks to research on a system which can automatically read product information during checkout. Silver told his friend Norman Joseph Woodland about the request, and they started working on a variety of systems. The basic idea was to use an optical device which responds to light/dark transition of the code. Although the idea was born in 1948 it took another 26 years before barcodes became commercially successful for automate supermarket checkout systems. The very first scanning of the now ubiquitous Universal Product Code (UPC) barcode was on a pack of Wrigley Company chewing gum in June 1974. The breakthrough became only possible due to the invention of the laser, especially the Helium Neon laser emitting a visible and continuous red beam. The use of laser light with optical and mechanical scanner made it possible to read the bar code under nearly all directions of observation which is written on an object. Another key component for the success of the barcode reader has been the upcoming computer. Once the scanned information is present as a modulated electronic signal, it has to be decoded, stored and displayed. After the successful and useful implementation in supermarkets the idea of barcode identification was used for postal application, tagging of patients in medical treatments, luggage tagging in air transportation and a lot more. This experiment makes use of a modified regular cash desk scanner to introduce this exciting technology. All major components are made accessible like the rotating polygon mirror, beam distribution mirror and receiver optics. The analogue optical signal is tapped and made available via BNC jacks to be displayed on an oscilloscope. A set of different enlarged barcodes are used to track the chain from the analogue to the digital signal conversion. By means of a set of black beam blocker the beam bender mirror are blinded to obtain only one scanning line to facilitate the interpretation of the optical signal. The scanner is connected via its USB bus to a computer where the received code is encoded and displayed. The software uses an attached database to identify already known scanned object or store newly scanned ones. A variety of own barcodes can be created and if required printed to own labels.

By using an own created EAN 8 bar code symbol card with the label “00000000” the signals of the bar code scanner are stored on the oscilloscope as shown in Fig. 2.47. For this purpose the raw signals of the scanner which are accessible at the rear of the scanner via BNC jacks are connected to the oscilloscope. The lower trace (yellow) shows the analog photodetector signal and the upper one (turquoise) shows the digital converted analog signal. On top of the Fig. 2.47 the corresponding bar code is shown. It can be seen that besides the desired signal other peaks exists, which are originating from the edges of the bar code label. To determine the beginning and end of the bar code start and stop signals provided by the barcode.

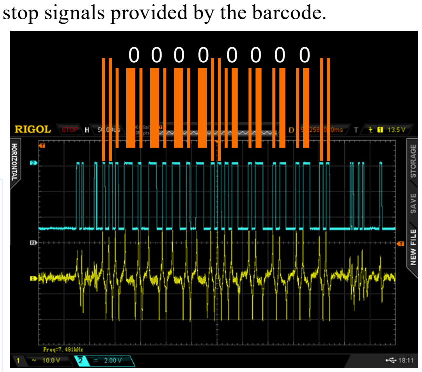

Fig. 2.47: EAN8 code with label “00000000”

Once such a signal appears, the evaluation electronic starts to look for the further signal and if the encoding fits into a defined frame including the stop signal, the content of the reading buffer is transferred to the USB bus.

LM-0800 Barcode Reader consisting of:

Item	*Code*	*Qty.*	*Description*	*Details page*
1	CA-0050	1	Set of tools and connection cable	127 (9)
2	CA-0450	2	BNC connection cable 1 m	130 (28)
3	ES-0400	1	Barcode scanner software	
4	OM-1000	1	Barcode scanner	117 (47)
5	OM-1010	1	Configuration bar code symbol cards	117 (48)
6	OM-1020	1	Barcode sample cards	117 (49)
7	OM-1030	1	Set of beam blocker cards	117 (50)
8	UM-LM08	1	Manual Barcode Reader	
	Required Option (order separately)			
9	CA-0120	1	Tablet PC Windows	128 (15)
10	CA-0200	1	Oscilloscope 100 MHz digital, two channel	129 (19)